HOKKAIDO UNIVERSITY

Title	ALIEN INVASION INTO THE BUFFER ZONE BETWEEN TWO COMPETING SPECIES
Author(s)	Ei, Shin-Ichiro; Ikeda, Hideo; Ogawa, Toshiyuki
Citation	Discrete and continuous dynamical systems. Series B, 28(12), 6034-6063 https://doi.org/10.3934/dcdsb.2023081
Issue Date	2023-12
Doc URL	https://hdl.handle.net/2115/93901
Rights	This is a pre-copy-editing, author-produced PDF of an article accepted for publication in Discrete and Continuous Dynamical Systems - B following peer review. The definitive publisher-authenticated version ALIEN INVASION INTO THE BUFFER ZONE BETWEEN TWO COMPETING SPECIES is available online at: http://dx.doi.org/10.3934/dcdsb.2023081
Type	journal article
File Information	EIO_final.pdf

Hokkaido University Collection of Scholarly and Academic Papers : HUSCAP

Manuscript submitted to
AIMS' Journals
Volume **X**, Number **0X**, XX **200X**

doi:10.3934/xx.xx.xx.xx

pp. **X–XX**

ALIEN INVASION INTO THE BUFFER ZONE BETWEEN TWO COMPETING SPECIES

Shin-Ichiro Ei

Department of Mathematics, Faculty of Science
Hokkaido University
Sapporo, 060-0810 Japan

Hideo Ikeda

Department of Mathematics
University of Toyama
Gofuku 3190, Toyama, 930-8555, Japan

Toshiyuki Ogawa

Graduate School of Advanced Mathematical Sciences
Meiji University
Nakano 4-21-1, Tokyo, 164-8525, Japan

Dedicated to the memory of Professor Masayasu Mimura

Abstract. Bifurcation of non-monotone traveling wave solutions of the three-species Lotka-Volterra competition diffusion system under strong competition is studied. The well-known front and back traveling wave formed by two species may lose its stability by the effect of third species and, as a result, allows the invasion. To discuss how the invasion is possible, stability change with respect to the intrinsic growth rate for the alien species are studied. Both numerical and theoretical bifurcation analysis around the bifurcation point reveal how the invasion affects the segregation of the original two species.

1. **Introduction.** Coexistence of different species is a key issue in mathematical ecology for understanding biodiversity. If we would like to see coexistence in a competitive system, spatial segregation is important, since we know Gause's law of competitive exclusion. There have been a lot of studies on two-species competition-diffusion system of Lotka-Volterra type:

$$\begin{cases} u_t = & d_1 u_{xx} + u(r_1 - a_1 u - b_{12} v), \\ v_t = & d_2 v_{xx} + v(r_2 - b_{21} u - a_2 v), \end{cases} \tag{1}$$

where $u(t,x)$ and $v(t,x)$ are the population densities of species U and V, respectively, at time $t > 0$ and position x in a bounded domain Ω under zero-Neumann boundary conditions.

2010 *Mathematics Subject Classification.* Primary: 35B32, 35B35, 35K55, 35K57; Secondary: 35Q92.

Key words and phrases. competitor-mediated coexistence, traveling wave solution, three-component competition-diffusion system, center manifold reduction, transcritical bifurcation.

The first author is supported in part by JSPS KAKENHI Grant Number JP22H01129. The second author is supported in part by JSPS KAKENHI Grant Numbers JP15K04995 and JP19K03618. The third author is supported in part by JSPS KAKENHI Grant Numbers JP17K05375 and JP20K03739.

When the constants $d_1, d_2, r_1, r_2, a_1, a_2, b_{12}, b_{21}$ are all positive it is known that the stable attractor consists of equilibrium solutions (see [8]). Therefore non-negative equilibrium solutions are important to understand the asymptotic behavior of (1). It is also known that any spatially non-constant equilibrium solution is unstable if the domain Ω is convex (see [12]). In the strong competition case: $a_2/b_{12} < r_2/r_1 < b_{21}/a_1$ there are two stable constant equilibria: $(r_1/a_1, 0), (0, r_2/a_2)$. So the general theory says that almost all the solutions finally converge to one of these constant equilibria. That is to say, competitive exclusion occurs. However, before converging to these final states, spatial temporary segregation of two species occurs depending on the initial conditions. We can also observe dynamical change of these segregated territories where the moving boundary between the territories is called the *buffer zone*. We remark that the two species face each other across the buffer zone. One may ask which direction the buffer zone is moving. If we consider the one dimensional problem, the velocity of traveling wave solutions to (1) is a key factor in deciding which species is superior.

A solution $(u(t,x), v(t,x))$ of (1) is called a traveling wave when it depends only on the traveling coordinate $z = x - \theta t$ for a constant velocity θ. It satisfies the following equations:

$$\begin{cases} d_1 u_{zz} + \theta u_z + u(r_1 - a_1 u - b_{12} v) = 0, \\ d_2 v_{zz} + \theta v_z + v(r_2 - b_{21} u - a_2 v) = 0. \end{cases} \tag{2}$$

Since we are interested in traveling waves which connect the two territories occupied by different species U and V, we impose the following boundary conditions.

$$\begin{cases} \lim_{z \to -\infty} (u(z), v(z)) = (0, r_2/a_2)\,, \\ \lim_{z \to +\infty} (u(z), v(z)) = (r_1/a_1, 0)\,. \end{cases} \tag{3}$$

It is known in [9] that non-negative traveling wave solutions exist uniquely and are asymptotically stable. We call this traveling wave solution UV-TW throughout this paper. It is, however, not so easy to determine the velocity, except for a few known results. The symmetric case is one of simplest examples, where we know the velocity is 0. Here, we say the equations are symmetric with respect to U and V if they do not change upon replacing u and v.

In this paper we will consider that the buffer zone actually provides a chance for an alien species, which are weaker than the other two, to invade. To do this, we consider the following three-component competition-diffusion system:

$$\begin{cases} u_t = & d_1 u_{xx} + u(r_1 - a_1 u - b_{12} v), \\ v_t = & d_2 v_{xx} + v(r_2 - b_{21} u - a_2 v), \\ w_t = & d_3 w_{xx} + w(r - b_{31} u - b_{32} v - a_3 w), \end{cases} \tag{4}$$

where $u(t,x), v(t,x)$ and $w(t,x)$ are the population densities of U, V and the alien species W at time $t > 0$ and position $x \in \mathbb{R}$, respectively. Suppose again that all the contants are positive and $a_2/b_{12} < r_2/r_1 < b_{21}/a_1$ so that the (u,v)-subsystem is strongly competing and has a UV-TW solution. It is clear that UV-TW solution also solves (4) in the case $w = 0$. We call this traveling wave solution UV0-TW to emphasize it is a solution for the three-component system (4). We assume the alien species W is weaker than U and V, that is, both $r/b_{31} < r_1/a_1$ and $r/b_{32} < r_2/a_2$ hold. By this assumption the alien species W can not invade the segregated territories or the tail part of UV0-TW. Then how about the buffer zone?

Let us examine the following case as a simple example:

$$\begin{cases} u_t = & u_{xx} + u(1-u-8v), \\ v_t = & v_{xx} + v(1-8u-v), \\ w_t = & d_3 w_{xx} + w(r-u-v-w). \end{cases} \tag{5}$$

Since the parameters are symmetric with respect to U and V, UV0-TW is a stationary solution and we call it UV0-SS to distinguish it from the original stationary solution UV-SS or UV-TW. Now, UV0-SS connects two equilibria $(1,0,0), (0,1,0)$ as $x \to \pm\infty$. Let us fix their phase so that they are symmetric with respect to the origin: $u(t,x) = v(t,-x)$. Notice that the stability of this UV0-SS is not induced by the fact that UV-SS is asymptotically stable in the two-component system. In fact, time-evolution simulations of (5) suggest there is a critical point $r = r_0$ for stability in the sense that this UV0-SS is asymptotically stable when $r < r_0$, while it is unstable when $r > r_0$. We also observe a stationary solution instead when $r > r_0$. The w-profile of this is not 0 but positive and has a single localized peak at $x = 0$. See Figure 1 for the profile of this stationary solution. We call this new stationary solution UVP-SS which means the w-profile of this is positive (P). If we decrease r then the peak of w also decreases until it attains $w = 0$ at the critical point r_0. Figure 1 suggests that the instability of UV0-SS gives rise to a bifurcation of UVP-SS. This means the alien species W succeeds to invade the buffer zone with a small investment. The numerical bifurcation diagram also suggests that there is another type of stationary solution nearby which has a negative w-profile. We call this UVN-SS in a similar way as above. Although this UVN-SS may not have an ecological meaning we can not ignore it if we are to totally understand the bifurcation structure around the critical point. The purpose of this study is to give the theoretical support for this bifurcation. However, let us admit it for the moment and think about the following related problem.

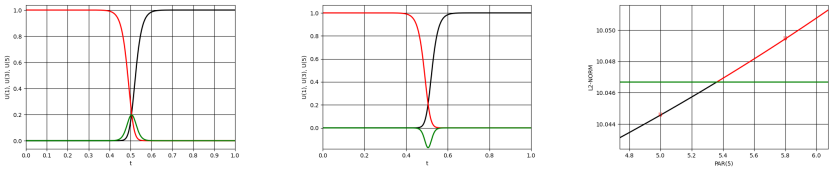

FIGURE 1. Profiles of UVP-SS (left) and UVN-SS (middle) for the system (5) with $d_3 = 1/10$ at the parameter values $r = 5.8$ and $r = 5.0$, respectively. Bifurcation diagram with respect to r (right).

In the three-component competition-diffusion system (5) the equations for U and V do not include feedback from W. Therefore even if this original U, V species allows the invasion of the alien species W, that means UV0-SS switches to UVP-SS, the original (u, v)-profile of UV0-SS does not change at all. It is, however, natural to consider the existence of inter-species interactions to U and V back from W. Let us just consider the following simplest case, where there are the same inter-species interactions from W to both U and V (suppose $b_{13} = b_{23} = \beta$ first):

$$\begin{cases} u_t = & u_{xx} + u(1-u-8v-b_{13}w), \\ v_t = & v_{xx} + v(1-8u-v-b_{23}w), \\ w_t = & d_3 w_{xx} + w(r-u-v-w). \end{cases} \tag{6}$$

We can observe that a similar bifurcation takes place if the inter-species coefficient $\beta > 0$ is sufficiently small. On the contrary, it turns out that UVP-SS loses its stability if β increases. We can observe, in time-evolution simulations of (6), that UV0-SS splits into two traveling waves that separate on both sides. Figure 2 shows the bifurcation diagrams for both cases. This suggests two facts. First, the bifurcation point r_0 does not depend on β. Second, there is a critical point $\beta^* \approx 4.25$ such that the bifurcation structure is *super-critical* when $\beta < \beta^*$, and *sub-critical* when $\beta > \beta^*$. Here, we call the bifurcation *super-critical* when we observe UVP-SS for $r > r_0$. In this case, UVP-SS becomes stable due to the exchange of stability. On the contrary, *sub-critical* means we observe UVP-SS for $r < r_0$. We would like to explain these facts as well in the later sections. At present, we can conclude from numerical simulations that UVP-SS is stable in the super-critical case, while it is unstable and plays the role of a separator between the stable UV0-SS and double traveling fronts moving forwards $\pm\infty$. See the schematic in Figure 3.

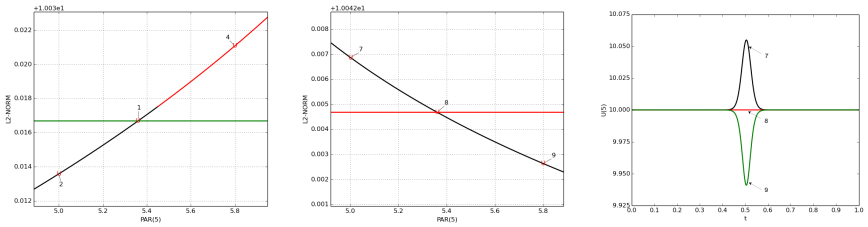

FIGURE 2. Both super-critical (left) and sub-critical (right) bifurcation structures are observed in the system (6) when $\beta = 2.0$ and $\beta = 8.0$, respectively. The horizontal line corresponds to UV0-SS and the crossing point is the bifurcation point to UVP-SS or UVN-SS. The upper part of the brach corresponds to UVP-SS. w-profiles for $\beta = 8.0$ with $r = 5, 5.359, 5.8$ are shown in the right figure.

In general, we will consider three-component competition-diffusion system:

$$\begin{cases} u_t = & d_1 u_{xx} + u(r_1 - a_1 u - b_{12} v - b_{13} w), \\ v_t = & d_2 v_{xx} + v(r_2 - b_{21} u - a_2 v - b_{23} w), \\ w_t = & d_3 w_{xx} + w(r - b_{31} u - b_{32} v - a_3 w). \end{cases} \tag{7}$$

We also write the same equations as follows:

$$\mathbb{U}_t = D\mathbb{U}_{zz} + c\mathbb{U}_z + \mathbb{F}(\mathbb{U}; r) \tag{8}$$

where $\mathbb{U} = {}^t(u, v, w)$, $D = \mathrm{diag}(d_1, d_2, d_3)$ and

$$\mathbb{F}(\mathbb{U}; r) = \begin{bmatrix} u(r_1 - a_1 u - b_{12} v - b_{13} w) \\ v(r_2 - b_{21} u - a_2 v - b_{23} w) \\ w(r - b_{31} u - b_{32} v - a_3 w) \end{bmatrix}.$$

Under the same assumptions there is a UV0-TW solution for an arbitrary r. Now we may ask again if there is a critical point $r = r_0$ for the stability. And if the UVP-TW solution bifurcates, how does the invasion of the alien species affect the original traveling wave? We show in Figure 4 the behavior of UVP-SS to (6) by adding different feedbacks from W: $b_{13} \neq b_{23}$. By the effect of the W species invasion, the original UV-SS stationary solution loses its symmetry and becomes a traveling wave solution if $b_{13} \neq b_{23}$. More generally, it can be said that the alien

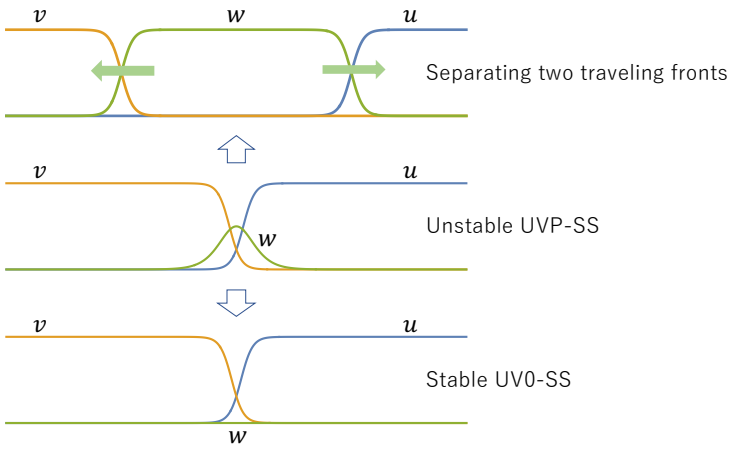

FIGURE 3. UVP-SS is unstable and plays the role of a separator between the stable UV0-SS and double traveling fronts moving towards $\pm\infty$.

invasion changes the velocity of the original UV-TW solution, as well as its profile. In fact, Chen, Hung, Mimura and Ueyama [4] obtained UVP-TW solutions to (7) exactly expressed for particular parameter sets. They also numerically showed that the velocity of the UVP-TW solution is different from that of the original UV-TW solution. They even found the parameter set where both UV0-TW and UVP-TW solutions are stable. However, their exact solutions are obtained only on a thin set of parameters and nothing is known about the bifurcation from UV0-TW. On the other hand, Chang et.al. [3] studied the existence and stability of UVP-TW solution by using the sub-and super-solution approach and perturbation theory for sufficiently small b_{13} and b_{23}. Chang et.al. [2] also constructed UVP-TW by gluing two different front traveling waves from U to W and from W to V. The local bifurcation structure for r is, however, still unclear.

We first study the stability of UV0-TW solution when $b_{13} = b_{23} = 0$. It turns out that this results in a scalar eigenvalue problem for equation w.

$$L_3(r)w = w'' + (r - b_{31}U(z) - b_{32}V(z))w = \lambda w.$$

Since there is no feedback from w, the UV-TW solution can be considered as just preparing the moving environment for the W species. Berestycki et. al. [1] has studied the unique existence of non-trivial solutions of this type of scalar equation when r is larger than a critical value. Their result can thus characterize a global aspect of the non-trivial traveling wave solutions. Here we are going to characterize UVP-TW in the bifurcation theory. This makes it possible to construct UVP-TW even when there is feedback from W. Moreover we will understand the rich bifurcation structure when it becomes the three-component system.

The paper is organized as follows. In §2, we recall the basic properties of UV-TW to the two-component competition-diffusion system. In §3, we study the linearized eigenvalue problem of the three-component competition-diffusion system around UV0-TW. Particularly, in §3.1 we consider a scaler eigenvalue problem, which corresponds to the third component of the above eigenvalue problem. In §3.2, we show the stability of UV0-TW, and in §3.3 we classify the degeneracy at the bifurcation

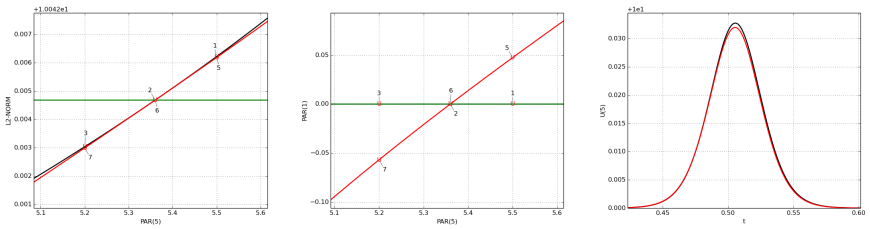

FIGURE 4. Compare the bifurcation structures to (6) by taking different inter-species interactions from W with $(b_{13}, b_{23}) = (2.0, 2.0), (4.0, 0.0)$. The two figures are bifurcation diagrams for UV0-SS, UVP/N-SS and UVP/N-TW with bifurcation parameter r. Vertical axes denote the peak height of the w-profile (left) and velocity (center), respectively. The green line and red curve correspond UV0-SS UVP/N-TW, respectively. UVP/N-SS is drawn by a black curve in the left diagram, while it is on the 0-velocity line in the center diagram. The w-profile for both UVP-SS(1) and UVP-TW(5) are drawn in the right figure.

point into two cases: generic and non-generic. In §4, we prepare typical examples where the scaler eigenvalue problem around UV-TW has the desired criticality. Corresponding to the two cases discussed in §4, different types of numerical bifurcation diagrams are shown in §5. In §6, we summarize the center manifold reduction to our problem and a reduced ODE system (normal form) which describes the wave dynamics of the bifurcated solution. We confirmed that the local bifurcation structures obtained in §5 are completely consistent with the normal form dynamics. Moreover, we found that the parameter space for (b_{13}, b_{23}) is divided into four different regions which characterize the bifurcation structures of UVP-TW. We also make a short notice on the global bifurcation structure of UVP-TW in §6.

2. **Traveling wave solutions to a two-component competition-diffusion system.** Let us consider the following two-component competition system:

$$\begin{cases} u_t = d_1 u_{zz} + c u_z + u(r_1 - a_1 u - b_{12} v), \\ v_t = d_2 v_{zz} + c v_z + v(r_2 - b_{21} u - a_2 v). \end{cases} \tag{9}$$

This is a sub-system of (7) by restricting $w = 0$. Here we assume that (9) is the case of strong competition, that is,

$$(A1) \qquad \frac{a_2}{b_{12}} < \frac{r_2}{r_1} < \frac{b_{21}}{a_1}.$$

This means that the competitions between species is sufficiently strong so that the coexisted state is unstable. In other words, the system is exclusive and only one species can survive. For this system, Kan-on gave the following results about the existence and stability of traveling wave solutions connecting two stable constant states ${}^t(0, r_2/a_2)$ and ${}^t(r_1/a_1, 0)$:

Lemma 2.1. (*Kan-on* [9]) *Under the assumption (A1), there uniquely exists* $c \in \mathbf{R}$ *such that (9) with boundary conditions* ${}^t(u, v)(-\infty, t) = {}^t(0, r_2/a_2), {}^t(u, v)(+\infty, t) =$

${}^t(r_1/a_1, 0)$ *has a strictly monotone positive stationary solution* ${}^t(U(z), V(z))$ *satisfying* $U_z(z) > 0, V_z(z) < 0$*, which corresponds to a traveling wave solution with the velocity* c*.*

Define a linearized operator L of (9) around ${}^t(U(z), V(z))$ by

$$L\begin{bmatrix} u \\ v \end{bmatrix} \equiv \begin{bmatrix} d_1 u_{zz} + cu_z + (r_1 - 2a_1U(z) - b_{12}V(z))u - b_{12}U(z)v \\ d_2 v_{zz} + cv_z - b_{21}V(z)u + (r_2 - b_{21}U(z) - 2a_2V(z))v \end{bmatrix}. \tag{10}$$

Lemma 2.2. (*Kan-on et al* [10]) *Under the assumption (A1), the essential spectrum of* L *is strictly contained in the left half-complex plane. Moreover, there exists* $\mu_0 > 0$ *such that isolated eigenvalues of* L *on the region* $\{\lambda \in \mathbb{C} \mid \mathrm{Re}\lambda > -\mu_0\}$ *is only* 0*, which is simple and the associated eigenfunction is* ${}^t(U_z(z), V_z(z))$*. Then,* ${}^t(U(z), V(z))$ *is asymptotically stable except for the translation.*

For the later use, we define an adjoint operators L^* of L by

$$L^*\begin{bmatrix} u \\ v \end{bmatrix} \equiv \begin{bmatrix} d_1 u_{zz} - cu_z + (r_1 - 2a_1U(z) - b_{12}V(z))u - b_{21}V(z)v \\ d_2 v_{zz} - cv_z - b_{12}U(z)u + (r_2 - b_{21}U(z) - 2a_2V(z))v \end{bmatrix} \tag{11}$$

and prepare the following lemma:

Lemma 2.3. (*Kan-on et al* [11]) *Any non-trivial bounded solution* ${}^t(u^*(z), v^*(z))$ *of* $L^{*t}(u, v) = {}^t(0, 0)$ *satisfies* $u^*(z)v^*(z) < 0$ *for all* $z \in \mathbf{R}$*.*

3. Linearized eigenvalue problem of a three-component competition-diffusion system.

${}^t(U(z), V(z), 0)$ is clearly a solution of the three-component system (8). Define a linearized operator $\mathcal{L}(r)$ around the solution ${}^t(U(z), V(z), 0)$ by

$$\mathcal{L}(r)\mathbb{U} \equiv \begin{bmatrix} d_1 u_{zz} + cu_z + (r_1 - 2a_1U(z) - b_{12}V(z))u - b_{12}U(z)v - b_{13}U(z)w \\ d_2 v_{zz} + cv_z - b_{21}V(z)u + (r_2 - b_{21}U(z) - 2a_2V(z))v - b_{23}V(z)w \\ d_3 w_{zz} + cw_z + 0 \cdot u + 0 \cdot v + (r - b_{31}U(z) - b_{32}V(z))w \end{bmatrix}. \tag{12}$$

Notice that the linearized eigenvalue problem

$$\mathcal{L}(r)\mathbb{U} = \lambda\mathbb{U} \tag{13}$$

will be decomposed into the scaler eigenvalue problem:

$$d_3 w_{zz} + cw_z + (r - b_{31}U(z) - b_{32}V(z))w = \lambda w \tag{14}$$

and the two-component system :

$$(\lambda I - L)\begin{bmatrix} u \\ v \end{bmatrix} = \begin{bmatrix} -b_{13}U(z)w \\ -b_{23}V(z)w \end{bmatrix}, \tag{15}$$

where L is defined in (10). Note that ${}^t(U(z), V(z), 0)$ is independent of the parameters $r, b_{13}, b_{23}, b_{31}$ and b_{32} which characterize the interaction between the existing species U, V and the alien species W.

3.1. Eigenvalue problem of the single equation (14).

Define a linear operator

$$L_3(r)w \equiv d_3 w_{zz} + cw_z + (r - b_{31}U(z) - b_{32}V(z))w \tag{16}$$

and consider an eigenvalue problem $L_3(r)w = \lambda w$ on the space $L^2(\mathbf{R})$. We assume the followings:

(A2) There exists $r = r_0 > 0$ such that $L_3(r)$ has the simple maximal eigenvalue 0.
(A3) The critical value r_0 above satisfies $r_0 - b_{31}r_1/a_1 < 0$ and $r_0 - b_{32}r_2/a_2 < 0$.

Assumption (A3) implies that the essential spectrum of $L_3(r_0)$ are strictly contained in the left half-complex plane.

Remark 3.1. The linear operator L_3 needs not to have any simple eigenvalue depending on the given functions $U(z), V(z)$ and the parameters b_{31}, b_{32}. We are going to give a sufficient condition where the assumptions (A2) and (A3) hold in section 4.

Here we define an eigenfunction $w(z)$ of $L_3(r_0)$ associated with eigenvalue 0 by $w_0(z)$ and we can assume $w_0(z)$ is positive without loss of generality.

Next let us consider an adjont operator of $L_3(r)$, which is defined by

$$L_3^*(r)w \equiv d_3 w_{zz} - cw_z + (r - b_{31}U(z) - b_{32}V(z))w. \tag{17}$$

We easily find that $L_3^*(r_0)$ also has simple eigenvalue 0 and an eigenfunction $w_0^*(z)$ of $L_3^*(r_0)$ associated with the 0-eigenvalue is represented as $w_0^*(z) \equiv e^{\frac{cz}{d_3}} w_0(z) > 0$ for $z \in \mathbf{R}$. We normalize w_0 and w_0^* satisfying $\langle w_0, w_0^* \rangle = 1$.

Finally, we consider a bifurcation problem of a single equation

$$w_t = d_3 w_{zz} + cw_z + (r - b_{31}U(z) - b_{32}V(z) - a_3 w)w \tag{18}$$

with the bifurcation parameter r. As we have mentioned in the introduction, the unique existence of non-trivial traveling wave to the scaler equation such as (17) is already studied by Berestyki et.al. [1]. However, let us give a brief proof of the existence of the bifurcation at this critical point $r = r_0$. Since $w = 0$ is a trivial solution for any positive r the leading order of the approximation of the solution is expressed by the 0-eigenfunction $w_0(z)$. Now let $r = r_0 + \eta$ and $w(z,t) = 0 + \theta(t)w_0(z) + \tilde{w}(z,t)$, where $\tilde{w}(\cdot,t) \in \{w_0\}^\perp$, i.e., $\langle \tilde{w}(\cdot,t), w_0^*(\cdot) \rangle = 0$ for $t > 0$, and substituting these into (18), we have

$$\tilde{w}_t = L_3(r_0)\tilde{w} - \dot{\theta} w_0 + \theta\eta w_0 + \eta\tilde{w} - a_3(\theta w_0 + \tilde{w})^2. \tag{19}$$

Then projecting (19) successively on $\{w_0\}$ and $\{w_0\}^\perp$ and using the relation $\langle w_0, w_0^* \rangle = 1$, we find an equation for $\theta(t)$

$$\dot{\theta} = \eta\theta - a_3\langle w_0^2, w_0^* \rangle \theta^2 + O(|\theta||\tilde{w}|| + ||\tilde{w}||^2) \tag{20}$$

and a quasilinear equation for $\tilde{w}(z,t)$

$$\begin{array}{rcl} \tilde{w}_t & = & L_3(r_0)\tilde{w} + O(|\theta|^2 + |\eta||\tilde{w}|| + |\theta||\tilde{w}|| + ||\tilde{w}||^2) \\ & = & L_3(r_0)\tilde{w} + O(|\theta|^2 + |\eta|^2 + ||\tilde{w}||^2). \end{array} \tag{21}$$

It is easy to see the existence of solutions $\tilde{w}$ of (21) and the relation $||\tilde{w}|| = O(|\theta|^2 + |\eta|^2)$. Then the dynamics of $\theta(t)$ is obtained as follows:

$$\dot{\theta} = \eta\theta - a_3\langle w_0^2, w_0^* \rangle \theta^2 + O(|\theta|^3 + |\theta||\eta|^2 + |\eta|^4). \tag{22}$$

Noting that $\langle w_0^2, w_0^* \rangle = \langle w_0^2, e^{\frac{cz}{d_3}} w_0 \rangle > 0$, we have a trans-critical bifurcation from the trivial solution $w = 0$ at $r = r_0$(i.e., $\eta = 0$). Although this discussion is only for the scaler equation (18), it is already a proof of the bifurcation of UVP/N-SS/TW from UV0-SS/TW for the system (4) and (5) since $a_3 > 0$ (See Fig 1). The main subject in this paper is, however, the bifurcation structure of UVP/N-TW for the general system (7) with $(b_{13}, b_{23}) \neq (0,0)$.

3.2. **Stability of UV0-TW of (8).** In this subsection, we want to examine the stability of UV0-TW solution ${}^t(U(z), V(z), 0)$ of (8) for $0 < r < r_0$.

Suppose that $0 < r < r_0$ and put $\lambda_0 = r - r_0 < 0$. Then, by Assumption (A2), we find that λ_0 is the maximal eigenvalue of $L_3(r)w = \lambda w$. This means that the eigenvalue problem $L_3(r)w = \lambda w$ has only trivial solution $w(z) = 0$ for $\lambda \geqq 0$. So, substituting this $w = 0$ into (15), we have

$$(\lambda I - L)\begin{bmatrix} u \\ v \end{bmatrix} = \begin{bmatrix} 0 \\ 0 \end{bmatrix}.$$

On the other hand, by Lemma 2.2, $(\lambda I - L)$ is invertible for $\lambda > 0$, which means ${}^t(u, v) = {}^t(0, 0)$. Thus we have the following theorem:

Theorem 3.2. *For any r satisfying $0 < r < r_0$, UV0-TW solution is stable.*

3.3. **Double 0-eigenvalue of the linearized operator $\mathcal{L}(r_0)$.** We easily find that for any $r > 0$, UV0-TW solution ${}^t(U(z), V(z), 0)$ has 0-eigenvalue on the eigenvalue problem (13), because an eigenfunction associated with the 0-eigenvalue is given by ${}^t(U_z(z), V_z(z), 0)$. Here we will show that the linearized eigenvalue problem (13) around the solution ${}^t(U(z), V(z), 0)$ has the double 0-eigenvalue at $r = r_0$.

First of all, define an adjoint operator $\mathcal{L}^*(r)$ of $\mathcal{L}(r)$ by

$$\mathcal{L}^*(r)\mathbb{U} \equiv \begin{bmatrix} d_1 u_{zz} - cu_z + (r_1 - 2a_1U(z) - b_{12}V(z))u - b_{21}V(z)v \\ d_2 v_{zz} - cv_z - b_{12}U(z)u + (r_2 - b_{21}U(z) - 2a_2V(z))v \\ d_3 w_{zz} - cw_z - b_{13}U(z)u - b_{23}V(z)v + (r - b_{31}U(z) - b_{32}V(z))w \end{bmatrix}. \tag{23}$$

For our purpose, we have to divide our discussion into the following two cases:

(I)	$\langle b_{13}Uu^* + b_{23}Vv^*, w_0\rangle \neq 0$	(generic),
(II)	$\langle b_{13}Uu^* + b_{23}Vv^*, w_0\rangle = 0$	(non − generic).

First we give the result about the generic case (I).

Theorem 3.3. (Generic case (I)) *At $r = r_0$, there exist an eigenfunction $\Phi(z)$ and an generalized eigenfunction $\Psi(z)$ satisfying $\mathcal{L}(r_0)\Phi(z) = 0$ and $\mathcal{L}(r_0)\Psi(z) = -\Phi(z)$, respectively. A similar results hold true for the adjoint operator $\mathcal{L}^*(r_0)$. That is, there exist an eigenfunction $\Phi^*(z)$ and an generalized eigenfunction $\Psi^*(z)$ satisfying $\mathcal{L}^*(r_0)\Phi^*(z) = 0$ and $\mathcal{L}^*(r_0)\Psi^*(z) = -\Phi^*(z)$, respectively.*

Since the proof of Theorem 3.3 is given in [7] so we omit it. However, here we only show the necessary information for Φ, Ψ, Φ^* and Ψ^* to compute the normal form coefficients in Section 6.3.

- $\Phi(z) = {}^t(U_z(z), V_z(z), 0)$.
- $\Psi(z) = {}^t(Q(z), c_1 w_0(z))$, where $Q(z)$ is a solution of

$$LQ(z) = {}^t(c_1 b_{13}U(z)w_0(z) - U_z(z), c_1 b_{23}V(z)w_0(z) - V_z(z))$$

and

$$c_1 = \frac{\langle {}^t(U_z, V_z), {}^t(u^*, v^*)\rangle}{\langle b_{13}Uu^* + b_{23}Vv^*, w_0\rangle}. \tag{24}$$

- $\Phi^*(z) = {}^t(0, 0, w_0^*(z))$.
- $\Psi^*(z) = {}^t(u^*(z)/\gamma, v^*(z)/\gamma, \hat{w}^*(z))$, where $\hat{w}^*(z)$ is a solution of

$$L_3^*(r_0)\hat{w}^*(z) = (b_{13}U(z)u^*(z) + b_{23}V(z)v^*(z))/\gamma - w_0^*(z)$$

and

$$\gamma = \langle b_{13}Uu^* + b_{23}Vv^*, w_0\rangle \neq 0. \tag{25}$$

Remark 3.4. Since we took the eigenfunction $w_0(z)$ of $L_3(r_0)$ positive, the sign of the third component of the generalized eigenfunction $\Psi(z)$ is determined by c_1.

Next we give the result about the non-generic case (II).

Theorem 3.5. (Non-generic case (II)) *At $r = r_0$, there exist eigenfunctions $\Phi(z)$ and $\Psi(z)$ satisfying $\mathcal{L}(r_0)\Phi(z) = 0$ and $\mathcal{L}(r_0)\Psi(z) = 0$, respectively. A similar results hold true for the adjoint operator $\mathcal{L}^*(r_0)$. That is, there exist eigenfunctions $\Phi^*(z)$ and $\Psi^*(z)$ satisfying $\mathcal{L}^*(r_0)\Phi^*(z) = 0$ and $\mathcal{L}^*(r_0)\Psi^*(z) = 0$, respectively.*

Since the proof of Theorem 3.5 is also given in [7] so we omit it. However, here we only show the necessary information for Φ, Ψ, Φ^* and Ψ^* to compute the normal form coefficients in Section 6.3.

- $\Phi(z) = {}^t(U_z(z), V_z(z), 0)$.
- $\Psi(z) = {}^t(Q(z), w_0(z))$, where $Q(z)$ is a solution of
$$LQ(z) = {}^t(b_{13}U(z)w_0(z), b_{23}V(z)w_0(z)).$$
- $\Phi^*(z) = {}^t(0, 0, w_0^*(z))$.
- $\Psi^*(z) = {}^t(u^*(z), v^*(z), \hat{w}^*(z))$, where $\hat{w}^*(z)$ is a solution of
$$L_3^*(r_0)\hat{w}^*(z) = b_{13}U(z)u^*(z) + b_{23}V(z)v^*(z).$$

Finally we note the followings:

Remark 3.6. Let Σ_1 be the spectrum of $\mathcal{L}(r_0)$ except for 0. Then, $\Sigma_1 \subset \{\lambda \in \mathbf{C} \mid Re\lambda < -\rho\}$ for some $\rho > 0$, because the essential spectrum of $\mathcal{L}(r_0)$ are strictly contained in the left half-complex plane by virtue of (A1) and (A3).

Remark 3.7. The non-generic condition (II) corresponds to a half line on the parameter space $B = \{(b_{13}, b_{23}) | b_{13} \geq 0, b_{23} \geq 0\}$ since $u^*(z)v^*(z) < 0$ by Lemma 2.3. Therefore the parameter space B is divided into two generic regions by this non-generic line.

4. Conditions which guarantee Assumptions (A2) and (A3).

The purpose of this section is to prepare the sufficient conditions for the existence of a simple eigenvalue of L_3 which is assumed in Assumptions (A2) and (A3). That is nothing but a possibility of localized invasion to the buffer zone. Although the sufficient conditions seems not to be optimal, we have at lease assured the meaningful bifurcation really occurs in the particular case of three-component competition system.

4.1. bound state property.

Let us consider the following Shrödinger operator:

$$L_\phi w := w'' + \phi(x)w$$

and its eigenvalue problem in the infinite interval:

$$w'' + \phi(x)w = \lambda w\ , \quad x \in \mathbb{R}. \tag{26}$$

We are interested in the potential function $\phi(x)$ where the corresponding Shrödinger operator has an eigenvalue in $L^2(\mathbb{R})$. When the Shrödinger operator has an eigenvalue we call its potential function has the **"bound state property"** .

We first take $\psi(x)$ which satisfies the following:

(A4) $\psi(x)$ is positive and decays exponentially to 0 as $x \to \pm\infty$.

Proposition 1. *If $\psi(x)$ satisfies the above property (A4) then $\phi(x) = s\psi(x)$ has the bound state property for sufficiently large positive number s. That means the eigenvalue problem (26) has an eigenvalue.*

Proof of Proposition 1. To prove this proposition we use the Strum-Liouville theory. First, an eigenvalue λ must be positive if (26) has an eigenfunction in $L^2(\mathbb{R})$. This is because (26) is written as follows

$$\begin{cases} w' = & z, \\ z' = & (\lambda - \phi(x))w, \end{cases} \tag{27}$$

and the eigenvalues and eigenvectors around $(0,0)$ at $x \to \pm\infty$ are $\pm\sqrt{\lambda}$ and $(1, \pm\sqrt{\lambda})$. Therefore, we have only to construct non-trivial solution which connects these eigenvectors at both ends. It is convenient to use the polar coordinate (ϱ, φ) to analyze (27). In fact the equation for the angle variable φ is as follows:

$$\varphi' = (\lambda - \phi(x) + 1)\cos^2\varphi - 1. \tag{28}$$

The angles $\pm\varphi^*$ which satisfies $\cos^2\varphi^* = 1/(1+\lambda)$ are the fixed points at $x \to \pm\infty$.

Now, let us fix a positive number λ. We can make the derivative of $-\varphi$ large enough for a certain interval $z \in (-R, R)$ by taking s large. Therefore we can find a non-trivial solution which connects $\pm\varphi^*$ by the shooting argument. Thus the proof of Proposition 1 is completed. □

Remark 4.1. The simple eigenvalue is positive by the assumption and the eigenfunction decays to 0 exponentially as $x \to \pm\infty$. Also the essential spectrum for L_ϕ is $(-\infty, 0)$.

Now, notice that the scaler eigenvalue problem (14) is equivalent to

$$d_3 p_{zz} + (r - b_{31}U(z) - b_{32}V(z) - \frac{c^2}{4d_3})p = \lambda p \tag{29}$$

by $p = we^{\frac{c}{2d_3}z}$. We can conclude from Proposition 1 that if $\psi(z) = r - b_{31}U(z) - b_{32}V(z)$ satisfies the property (A4) then (29) has an eigenvalue by taking d_3 small enough. This is simply because $1/d_3$ can play a role of scaling effect s in Proposition 1.

Remember that the traveling wave solution of the two-component system (9) connects two stable constant states $(\alpha, 0), (0, \beta)$ where $\alpha = r_1/a_1, \beta = r_2/a_2$. Take the line $l = \{(u, v) | \beta u + \alpha v = \alpha\beta\}$ passing through these constant states.

Proposition 2. *If $d_1 = d_2 (= d)$ then the heteroclinic orbit $\{(U(z), V(z)) | z \in \mathbb{R}\}$ is in the lower side of the line l. Therefore, $\psi(z) = \alpha\beta - \beta U(z) - \alpha V(z)$ satisfies the property (A4).*

Proof of Proposition 2. The proof is very simple. First, the traveling wave solution satisfies

$$\begin{aligned} -cU' &= dU'' + (r_1 - a_1 U - b_{12}V)U, \\ -cV' &= dV'' + (r_2 - b_{21}U - a_2 V)V. \end{aligned}$$

We have only to confirm $f(U(z), V(z)) = \beta U(z) + \alpha V(z) \le \alpha\beta$. If, on the contrary, suppose there was a point z such that $f(U(z), V(z)) = \beta U(z) + \alpha V(z) > \alpha\beta$. Then there is a point z^* which attains the maximum since $f(U(z), V(z))$ converges $\alpha\beta$ at both ends. Therefore, it holds that $\frac{df(U,V)}{dz}(z^*) = 0$. We can also show $\frac{d^2 f(U,V)}{dz^2}(z^*) > 0$ as follows and this leads to a contradiction.

Noticing the derivatives of this are

$$\frac{df(U(z),V(z))}{dz} = \beta U' + \alpha V'$$

and

$$\frac{d^2 f(U(z),V(z))}{dz^2} = \beta U'' + \alpha V'',$$

we have

$$\begin{aligned} &d \cdot (\beta U''(z^*) + \alpha V''(z^*)) \\ &= -c(\beta U'(z^*) + \alpha V'(z^*)) - (r_1 - a_1 U - b_{12} V)\beta U - (r_2 - b_{21} U - a_2 V)\alpha V \\ &= -\beta(r_1 - a_1 U(z^*) - b_{12} V(z^*))U(z^*) - \alpha(r_2 - b_{21} U(z^*) - a_2 V(z^*))V(z^*). \end{aligned}$$

Since the maximum point $(U(z^*), V(z^*)))$ is in the upper side of the line l it also holds that $(r_1 - a_1 U(z^*) - b_{12} V(z^*)) < 0, (r_2 - b_{21} U(z^*) - a_2 V(z^*)) < 0$. Thus we have $\frac{d^2 f(U,V)}{dz^2}(z^*) > 0$ and this is a contradiction. Thus the proof of Proposition 2 is completed. □

To summarize we can conclude the following:

Proposition 3. *If $d_1 = d_2$ and $(r, b_{31}, b_{32}) = (\alpha\beta, \beta, \alpha)$ then the assumption (A2) is satisfied for sufficiently small d_3.*

Proof of Proposition 3. By Propositions 1 and 2 we have a positive eigenvalue λ^* to the following problem by taking d_3 small enough:

$$d_3 p_{zz} + (\alpha\beta - \beta U(z) - \alpha V(z))p = \lambda^* p. \tag{30}$$

This is equivalent to

$$d_3 p_{zz} + (\alpha\beta + \frac{c^2}{4d_3} - \lambda^* - \beta U(z) - \alpha V(z) - \frac{c^2}{4d_3})p = 0 \tag{31}$$

which means that p solves (29) with $r_0 = \alpha\beta + \dfrac{c^2}{4d_3} - \lambda^*$ and $\lambda = 0$. Thus the proof of Proposition 3 is completed. □

Remark 4.2. It should be remarked that Assumption (A3) is a direct consequence of Assumption (A2) in the special case when the traveling velocity $c = 0$. Since the eigenfunction needs to decay exponentially, the limit value of $r_0 - b_{31}U(z) - b_{32}V(z)$ should be negative as $z \to \pm\infty$. Thus, we have $r_0 - b_{31} r_1/a_1 < 0$ and $r_0 - b_{32} r_2/a_2 < 0$.

4.2. **Explicit representation of UV-TW and the scaler eigenfunction.** The second example is given by expressing the eigenfunction for $L_3(r_0)$ explicitly by using elementary functions. It is known that UV-TW solutions to the two-component competition system can be explicitly represented for certain parameter regimes ([13],[14]). In fact, if the parameters

$$d_1 = 1, \quad r_1 = 1, \quad a_1 = 1, \quad b_{12} = e,$$

$$d_2 = d, \quad r_2 = a, \quad b_{21} = b, \quad a_2 = 1,$$

satisfy $d = 1/3e, \quad b = 2 + 5a/3 - ae, \quad 1/e < a < b$ then the (a, e)-parameter families of TW solutions of (9) are given by

$$U(z) = \frac{1}{2}\left(1 + \tanh(sz)\right), \quad V(z) = \frac{a}{4}\left(1 - \tanh(sz)\right)^2$$

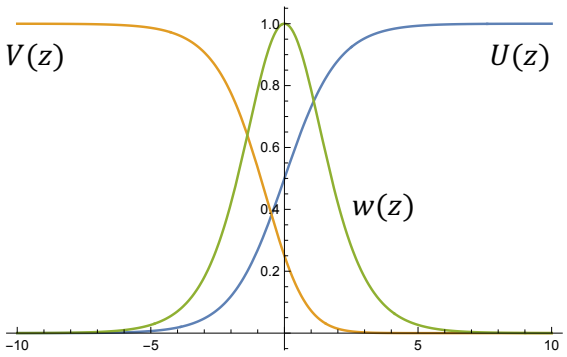

FIGURE 5. The exact traveling wave solution $(U(z), V(z))$ and the eigenfunction $w(z)$ when $a = 1, e = 2$.

where $s = \sqrt{2ae}/4, \quad z = x - ct, \quad c = (ae - 2)/\sqrt{2ae}$.

Now if moreover, the coefficients in the w-equation for (7) are

$$d_3 = 1, \quad b_{31} = 2(1 + ae), \quad b_{32} = 3e$$

then the scaler eigenvalue equation (14) becomes

$$w_{zz} + cw_z + w(r_3 - 2(1 + ae)U - 3eV) = 0$$

and it has the following non-trivial solution $w(z)$ at $r_3 = 1 + 2ae$:

$$w(z) = 1 - \tanh^2(sz).$$

Thus, this gives an explicit example which satisfy Assumption (A2) (See the profile in Figure 5). We can also confirm the assumption (A3) since the limit values

$$\lim_{z \to \pm\infty} (1 + 2ae - 2(1 + ae)U(z) - 3eV(z)) = \begin{cases} -1 \\ 1 - 2ae \end{cases}$$

are both negative.

5. **Bifurcation structure by numerical continuation.** We have discussed that there is a critical value $r = r_0$ for the growth rate of alien species under Assumptions (A2) and (A3). And we have given two examples of parameter sets for the equations (7) which satisfy these two assumptions. Of course, there are still so many variations of parameter set where the system (7) has the critical value. First, we start to introduce what we can typically observe by the numerical continuation of traveling wave solutions in the following subsection. And later subsections, we introduce the bifurcation diagrams corresponding to the above two examples where we proved the existence of the critical eigenvalue. And moreover, in later sections we will see these bifurcation diagrams are consistent with the theoretically obtained reduced ODE systems.

5.1. **Numerical continuation of traveling wave solutions.** According to [4] let us first consider the following parameter set in the system (7).

$$d_1 = 1, \quad r_1 = 1, \quad a_1 = 1, \quad b_{12} = 8,$$
$$d_2 = 23/24, \quad r_2 = 23, \quad b_{21} = 97/3, \quad a_2 = 23,$$
$$d_3 = 5/6, \quad b_{31} = 17, \quad b_{32} = 23, \quad a_3 = 1.$$

Notice that r plays a role of the bifurcation parameter in our study. This parameter set is convenient for our study in the following sense. First, the constrained (u, v) two-component system has the following exact representation for the UV-TW solution:

$$U(z) = \frac{1}{2}\left(1 + \tanh(z)\right), \quad V(z) = \frac{1}{4}\left(1 - \tanh(z)\right)^2 \tag{32}$$

where, $z = x - ct$, $c = 3/2$. Therefore, $(u, v, w) = P(z) = (U(z), V(z), 0)$ is also the traveling wave solution (UV0-TW) to (8) for an arbitral r and we can calculate at least one 0-eigenfunction exactly by the derivative of this. Second, the three-component system (8) also has the exact representation for UVP-TW wave solution with $c = 3/2$ when $r = 50/3$ and $b_{13} = b_{23} = 0$ as follows :

$$U(z) = \frac{1}{2}\left(1 + \tanh(z)\right), \quad V(z) = \frac{1}{4}\left(1 - \tanh(z)\right)^2, \quad W(z) = \frac{3}{4}\left(1 - \tanh^2(z)\right). \tag{33}$$

We can use this exact representation as the starting point for the numerical continuation. Notice that it is necessary to have an accurate traveling wave solution in such a case.

We use the package:HomCont(AUTO)[5] for the numerical continuation of traveling wave solutions. Here, we consider the problem as a stationary problem by using the traveling wave coordinate in the calculation by HomCont. Since the traveling wave solution has the trivial 0-eigenvalue, as we have already discussed, so the bifurcation is degenerate. And additionally, HomCont is calculating the heteroclinic orbit of the ODE. Therefore, HomCont is not able to detect $r = r_0$ as a bifurcation point. Therefore what we can do is as follows. First we take the exact representation of UVP-TW wave solution as the starting point for the continuation. Second, we observe the w-profile of the solution along the continuation branch. And if we find the point where $w \equiv 0$ along the branch and moreover the velocity of the traveling wave is equal to the UV0-TW wave, we would conclude this must be the bifurcation point which we are interested in. This is because we know the traveling wave solution which satisfy $w \equiv 0$ is unique. If the sign of w changes across this point, it will be a side note.

Also, notice that we have the exact representation of UVP-TW solution only for a specific parameters $(r, b_{13}, b_{23}) = (50/3, 0, 0)$. Therefore, first continuation should be calculated by taking (b_{13}, b_{23}) as bifurcation parameters from $(0, 0)$ to a particular values of (b_{13}, b_{23}) by fixing $r = 50/3$. And second continuation by r parameter is going to be what we are interested in.

Let us explain what we can observe by showing typical numerical result in Figure 6. Black curve and red line correspond to branches of the UVP-TW and UV0-TW solution, respectively. Notice that we show the L^2-norm (middle) $||w + 10||$ which almost correspond to the peak/bottom height of w. Since the UV0-TW solution satisfy $w \equiv 0$ it does not depend on r. Now, look at the solution at the point No.4 along the branch at the position $r = 16.162$. We notice that the w-profile of the solution is 0 and the velocity is equal to that of the UV0-TW at the point No.4. And, $w > 0$ for the solutions at No.1,2 and 3. While $w < 0$ for No.5,6 and 7. Moreover, we can numerically calculate the critical value $r_0 \approx 16.162$ for $L_3(r)$. We can thus numerically conclude that the point No.4 is the bifurcation point in which we are interested. And the w-positive solution appears for $r > r_0$ as a result of the bifurcation. We call this situation *super-critical*. On the other hand, if the w-positive solution appears for $r < r_0$, we call the bifurcation *sub-critical*. Although

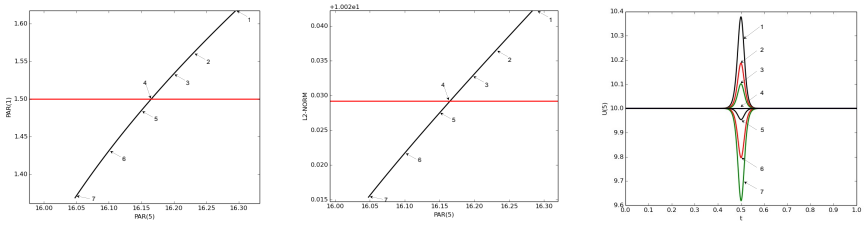

FIGURE 6. Bifurcation diagrams with respect to r when $(b_{13}, b_{23}) = (0.5, 0.5)$. Vertical axes denotes the velocity (left) and L^2-norm $||w + 10||$ (middle) of the traveling wave. The profiles $w(z) + 10$ of corresponding traveling wave solutions are also displayed (right).

the velocity of the UVP-TW is larger than that of the UV0-TW in this specific case, it could be smaller, as we will see later, depending on the parameters b_{13} and b_{23}. Thus it is necessary to observe the bifurcation diagram by $||w + 10||$, i.e., the peak/bottom hight of w, to see it is super-critical or sub-critical. Therefore we will show bifurcation diagrams both by the velocity and by $||w + 10||$ in the followings.

In this example, we have numerically confirmed that the critical value r_0 satisfies both (A2) and (A3). Therefore we will not proceed further study by this parameter set but instead, we will consider the following two cases where we have theoretical support for (A2) and (A3).

5.2. **Bifurcation from UV0-SS.** Let us consider the following systems (34) and (35) where the base two-component system is symmetric. These are the same as (5) and (6), respectively, which we have introduced in section 1.

$$\begin{cases} u_t = & u_{xx} + u(1 - u - 8v), \\ v_t = & v_{xx} + v(1 - 8u - v), \\ w_t = & dw_{xx} + w(r - u - v - w). \end{cases} \tag{34}$$

Since $d_1 = d_2 = 1$ and $(b_{31}, b_{32}) = (r_2/a_2, r_1/a_1) = (1, 1)$ in (34) we know from Proposition 3 that the scaler eigenvalue problem $L_3(r)$ has an eigenvalue in L^2 when d is sufficiently small. Assumption (A3) also holds true since UV-SS is a stationary solution (See Remark 4.2). Let us take $d = 1/10$ from now on. In fact, the critical value $r_0 \approx 5.359$ in this case. Notice that we don't have an exact representation of the UV-SS for this parameter set, we have used the numerical approximation for UV-SS to solve the eigenvalue problem $L_3(r_0)w = 0$. The HomCont continuation for UV0-SS and UVP-SS shows the super-critical bifurcation at r_0 as we already see in Figure 1. For the starting point of numerical continuations for UVP-SS as well as UV0-SS we use the exact representation (32) and (33) for the parameter set in the previous subsection.

We can also consider the case where there are feedback effects to U and V from W:

$$\begin{cases} u_t = & u_{xx} + u(1 - u - 8v - b_{13}w), \\ v_t = & v_{xx} + v(1 - 8u - v - b_{23}w), \\ w_t = & dw_{xx} + w(r - u - v - w). \end{cases} \tag{35}$$

First, let us consider the case $b_{13} = b_{23} = \beta$. We also set $d = 1/10$ to have the same critical point r_0 as (34). As we have already shown in Figure 2 the bifurcation

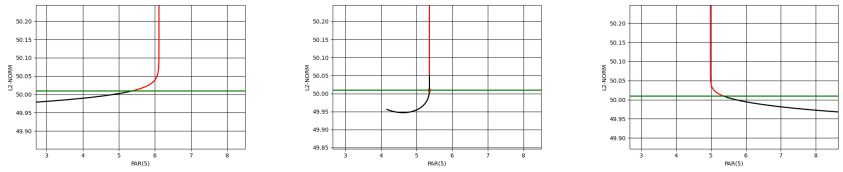

FIGURE 7. Bifurcation diagrams of UV0-SS(green), UVP-SS(red) and UVN-SS(black) for (35) with respect to r when $\beta = 3.2, 4.272, 5.0$(N1, N2, N3 in Figure 19) from the left. Vertical axes denotes L^2-norm $||w + 50||$ of the traveling wave. Transition point between super- and sub-critical bifurcation is approximately $\beta = 4.272$.

at the critical point is super-critical when the feedback effect $\beta < \beta^*$, and on the contrary, sub-critical when $\beta > \beta^*$. In fact, numerical continuation suggests the critical value $\beta^* \approx 4.272$. See also Figure 7 to see the transition before and after the critical value β^*. The point $(b_{13}, b_{23}) = (\beta, \beta)$ clearly satisfies the non-generic condition(II) by the symmetry. Therefore, it is on the non-generic line as in Remark 3.7. Thus we need to study what happens in the generic case(I), that is, if (b_{13}, b_{23}) is above/below the non-generic line.

Let us, next, choose $(b_{13}, b_{23}) = (\beta, 0)$ to study the generic case. As we have also shown in the introduction(Figure 4) the bifurcated solution is a traveling wave (UVP-TW) by the asymmetric feedbacks. Therefore we draw the bifurcation diagram not only by the L^2 measure but also the velocity of the traveling wave. See Figure 8. In both cases we can observe a transition of the bifurcation structure from super- to sub-critical similarly to the non-generic case. It is, however, remarkable that in both cases UVP-TW has positive velocity if (b_{13}, b_{23}) is below the non-generic line. Although we don't show the results when (b_{13}, b_{23}) is above the non-generic line the velocity is clearly negative. Another notable difference is that a saddle-node bifurcation is observed on the sub-critical branch of UVP-TW. And as a result, UVP-TW recovers its stability. In fact, we can observe bi-stability for both UV0-SS and UVP-TW even by the time-evolution simulation. Continuation results suggests that the width of bistable parameter region for r approaches 0 if we choose (b_{13}, b_{23}) closer to the non-generic line. (Also see Figure 23 in section 7.)

5.3. **The case where we have explicit representation of UV-TW and the scaler eigenfunction.** Now we choose the parameter set which we introduced in the subsection 4.2. Therefore, we have an explicit representation of the eigenfunction for $L_3(r_0)$ as well as UV-TW. Let us take $a = 1$ and $e = 2$. Then, the equations are the followings:

$$\begin{cases} u_t = & u_{xx} + u(1 - u - 2v - b_{13}w), \\ v_t = & \frac{1}{6}v_{xx} + v(1 - \frac{5}{3}u - v - b_{23}w), \\ w_t = & w_{xx} + w(r - 6u - 6v - w). \end{cases} \tag{36}$$

Moreover, UV-TW is expressed as

$$U(z) = \frac{1}{2}\left(1 + \tanh(z/2)\right), \quad V(z) = \frac{1}{4}\left(1 - \tanh(z/2)\right)^2$$

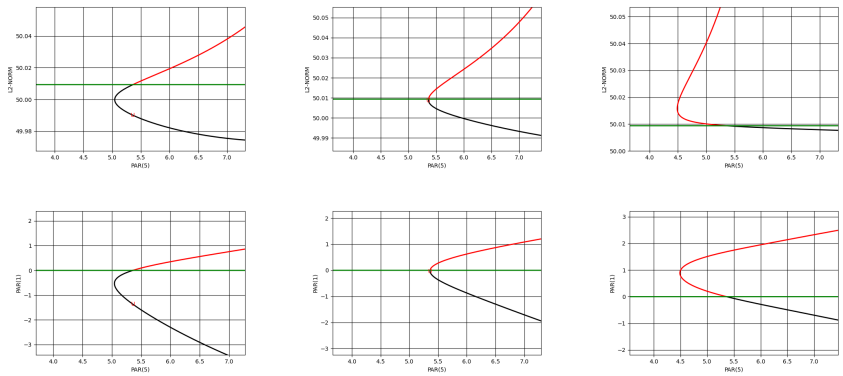

FIGURE 8. Bifurcation diagrams of UV0-SS(green), UVP-SS(red) and UVN-SS(black) for (35) with respect to r when $(b_{13}, b_{23}) = (\beta, 0)$ with $\beta = 5.6, 8.32, 12.0$(A1, A2, A3 in Figure 19) from the left. Vertical axes denotes L^2-norm $||w + 50||$ and the velocity of the traveling wave is displayed in the upper and lower columns, respectively. $\beta = 8.32$ is approximately the transition point.

where $z = x - ct$ with $c = 0$. Therefore, it is actually UV-SS. The scaler eigenvalue problem:

$$L_3(r)w \equiv w_{zz} + (r - 6U(z) - 6V(z))w \tag{37}$$

has 0-eigenvalue with the eigenfunction:

$$w(z) = 1 - \tanh^2(z/2).$$

at $r = r_0 = 5$. The non-generic line $\langle b_{13}Uu^* + b_{23}Vv^*, w_0\rangle = 0$ is also written as $b_{23} = \delta b_{13}$ where $\delta = -\langle Vv^*, w_0\rangle/\langle Uu^*, w_0\rangle \approx 0.929761$.

We observe the similar transition from super- to sub-critical bifurcation. In fact, here are three types of typical transitions by moving the points (b_{13}, b_{23}) along three lines: b_{13}-axis (Figures 9, 10), b_{23}-axis (Figures 11, 12) and the non-generic line $\{(\beta, \beta\delta)\}$ (Figures 13, 14). These sample points G1 through G9 are also displayed in Figure 21.

6. **Bifurcation analysis.** In the previous section we observe the bifurcation structure of the UVP/N/0-TW solutions to (7) by the numerical continuation. It is numerically confirmed that the trans-critical bifurcation takes place at the critical point $r = r_0$. Moreover, it is super-critical when $(b_{13}, b_{23}) \in \mathbb{R}^+ \times \mathbb{R}^+$ are close to $(0, 0)$. While it is sub-critical otherwise. One might wonder what separates these two different behaviors. The purpose of this section is to answer this question. To do that we are going to reduce the dynamics around the critical point as we partially studied in the case of the scaler equation (18). There, the critical eigenfunction w_0 plays a key role, while in this case, the linearized operator $\mathcal{L}(r_0)$ is degenerate and has two dimensional generalized eigenspace as we see in Section 3.3. Therefore we need to take into account the generalized eigenfunction Ψ (generic case) or the eigenfunction Ψ (non-generic case) as well as the eigenfunction $\Phi = P_z$. And we can obtain a two dimensional reduced dynamics which approximates the whole dynamics around the UV0-TW solution close to the critical point. Let us prepare the formulation as follows.

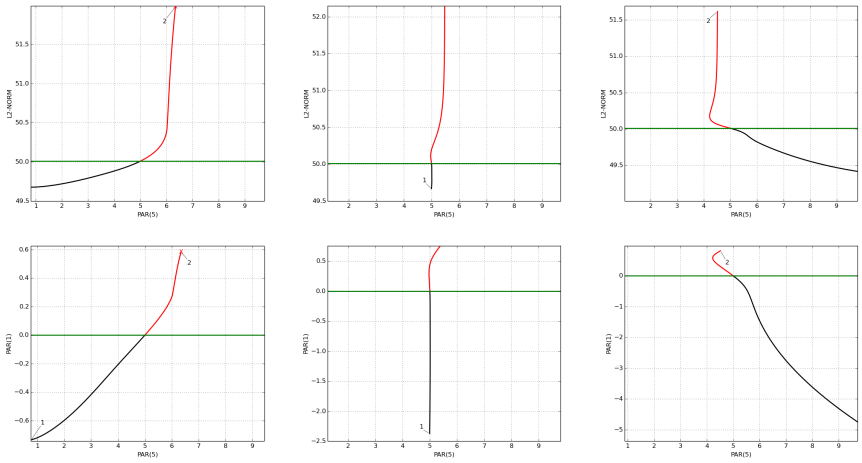

FIGURE 9. Bifurcation diagrams of UV0-SS(green), UVP-SS(red) and UVN-SS(black) for (36) with respect to r when $(b_{13}, b_{23}) = (\beta, 0)$ with $\beta = 0.16, 0.4, 0.8$(G1, G2, G3 in Figure 21) from the left. Vertical axes denotes L^2-norm $||w + 50||$ and the velocity of the traveling wave is displayed in the upper and lower columns, respectively. $\beta = 0.4$ is approximately the transition point.

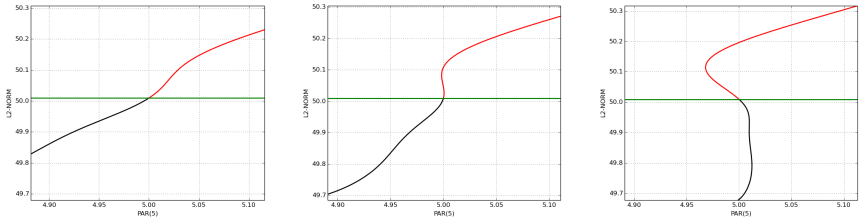

FIGURE 10. Enlarged view of the bifurcation diagrams for (36) with respect to r when $(b_{13}, b_{23}) = (\beta, 0)$ with $\beta = 0.384, 0.4, 0.416$ from the left.

6.1. **Reduction to a center manifold in the generic case.** We consider (8) in a neighborhood of $r = r_0$. For this purpose, we introduce a new parameter η such that $\eta = r - r_0$ and rewrite the equation (8) in a more convenient form

$$\mathbb{U}_t = \mathcal{P}(\mathbb{U}) + \eta \mathbb{G}(\mathbb{U}), \tag{38}$$

where $\mathcal{P}(\mathbb{U}) = D\mathbb{U}_{zz} + c\mathbb{U}_z + \mathbb{F}(\mathbb{U}; r_0)$ and $\mathbb{G}(\mathbb{U}) = {}^t(0, 0, w)$. We have seen that the following four conditions (H1) $\sim$ (H4) hold true in Section 3.

(H1) For any η, (38) has the traveling front solution $P(z) = {}^t(U(z), V(z), 0)$ with the velocity c.

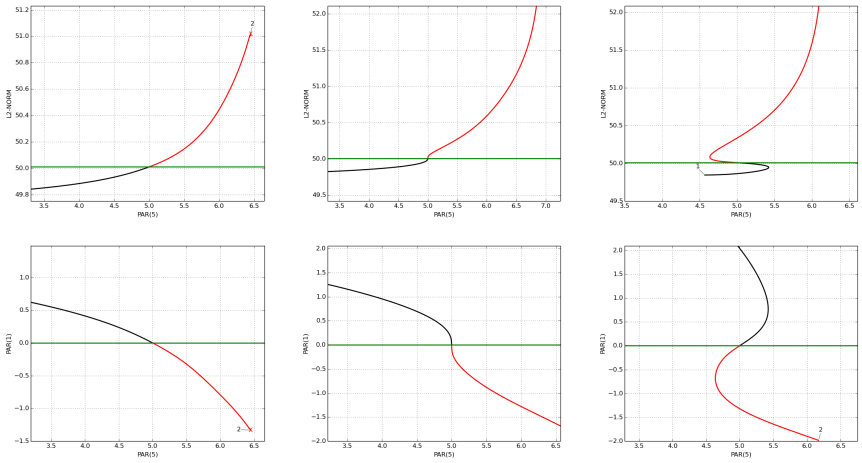

FIGURE 11. Bifurcation diagrams of UV0-SS(green), UVP-SS(red) and UVN-SS(black) for (36) with respect to r when $(b_{13}, b_{23}) = (0, \beta)$ with $\beta = 0.32, 0.69, 1.6$ (G4, G5, G6 in Figure 21) from the left. Vertical axes denotes L^2-norm $||w + 50||$ and the velocity of the traveling wave is displayed in the upper and lower columns, respectively. $\beta = 0.69$ is approximately the transition point.

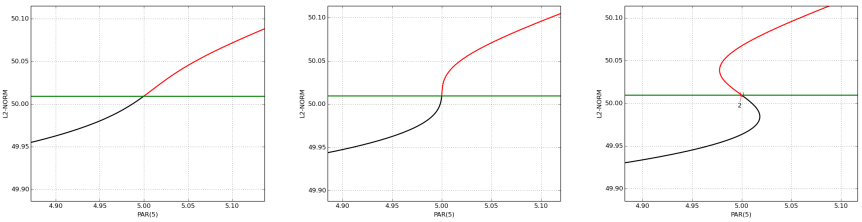

FIGURE 12. Enlarged view of the bifurcation diagrams for (36) with respect to r when $(b_{13}, b_{23}) = (0, \beta)$ with $\beta = 0.56, 0.69, 0.72$ from the left.

The linearized operator $\mathcal{L}(r_0)$ around $P(z)$ has the 0 eigenvalue, which comes from the translation invariance of $P(z)$. That is,

$$\mathcal{L}(r_0)P_z(z) = \mathbf{0} \text{ for } P_z(z) = {}^t(U_z(z), V_z(z), 0). \tag{39}$$

From now we assume the case (I), that is, $\langle b_{13}Uu^* + b_{23}Vv^*, w_0\rangle \neq 0$ for a while.

(H2) At $r = r_0$, there exists the generalized eigenfuntion $\Psi(z)$ of $\mathcal{L}(r_0)$ satisfying

$$\mathcal{L}(r_0)\Psi(z) = -P_z(z). \tag{40}$$

(H3) The spectrum Σ_1 of $\mathcal{L}(r_0)$ defined on $X \equiv (L^2(\mathbf{R}))^3$ except for 0 strictly contained in the left half-complex plane. That is, $\Sigma_1 \subset \{\lambda \in \mathbf{C} \mid Re\lambda < -\rho\}$ for some $\rho > 0$. (See Remark 3.6).

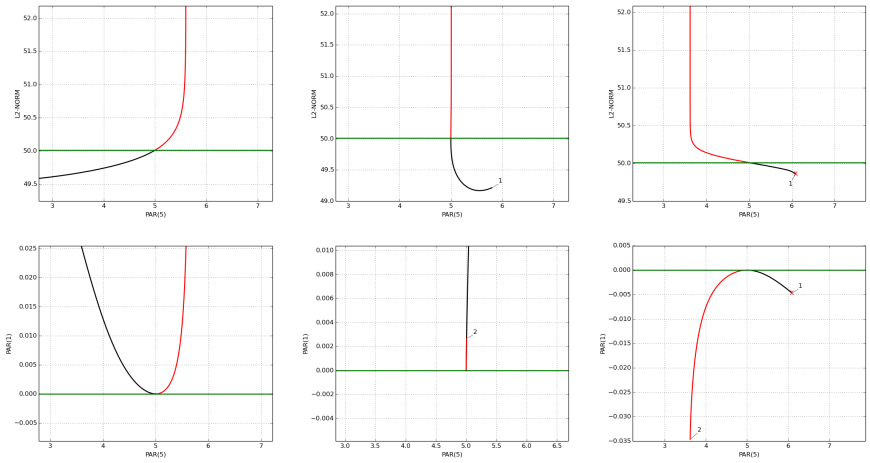

FIGURE 13. Bifurcation diagrams of UV0-SS(green), UVP-SS(red) and UVN-SS(black) for (36) with respect to r when $(b_{13}, b_{23}) = (\beta, \beta * 0.92976)$ with $\beta = 0.2, 0.25495, 0.5$ (G7, G8, G9 in Figure 21) from the left. Vertical axes denotes L^2-norm $||w + 50||$ and the velocity of the traveling wave is displayed in the upper and lower columns, respectively. $\beta = 0.25495$ is approximately the transition point.

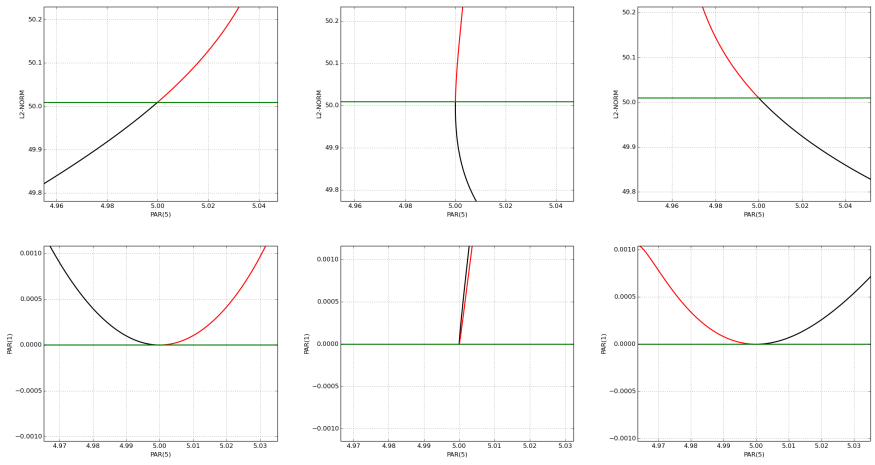

FIGURE 14. Enlarged view of the bifurcation diagrams for (36) with respect to r when $(b_{13}, b_{23}) = (\beta, \beta * 0.92976)$ with $\beta = 0.25, 0.25495, 0.26$ from the left. Vertical axes denotes L^2-norm $||w + 50||$ and the velocity of the traveling wave is displayed in the upper and lower columns, respectively.

(H4) For the adjoint operator $\mathcal{L}^*(r_0)$, there exist an eigenfuction $\Phi^*(z)$ and an generalized eigenfuction $\Psi^*(z)$ satisfying

$$\mathcal{L}^*(r_0)\Phi^*(z) = \mathbf{0}, \ \mathcal{L}^*(r_0)\Psi^*(z) = -\Phi^*(z). \tag{41}$$

We can show the following lemma:

Lemma 6.1. *Ψ, Φ^* and Ψ^* are uniquely determined by the normalization*

$$\langle P_z, \Psi\rangle = 0,\ \langle P_z, \Psi^*\rangle = 1,\ \langle \Psi, \Psi^*\rangle = 0. \tag{42}$$

For the proof see the appendix. Here we note

Remark 6.2.

$$\langle \Psi, \Phi^*\rangle = 1,\ \langle P_z, \Phi^*\rangle = 0$$

automatically hold true.

Under the conditions (H1), (H2), (H3) and (H4), we can consider the center manifold reduction as follows. Let Q and R be projections with respect to $\mathcal{L}(r_0)$ corresponding to the spectral sets $\{0\}$ and Σ_1, respectively. Moreover, define $E = QX$ and $E^\perp = RX$ where $R = I - Q$. Then we have $E = \mathrm{span}\{P_z, \Psi\}$, $E^\perp = \{\mathbb{U} \in X \mid \langle \mathbb{U}, \Phi^*\rangle = 0 = \langle \mathbb{U}, \Psi^*\rangle\}$ and $Q\mathbb{U} = \langle \mathbb{U}, \Psi^*\rangle P_z + \langle \mathbb{U}, \Phi^*\rangle \Psi$ for $\mathbb{U} \in X$. Furthermore let $S(z;\theta) \equiv P(z) + \theta\Psi(z)$ and define the translation operator τ by $(\tau(\ell)(\mathbb{U})(z) = \mathbb{U}(z - \ell)$. Put $\mathcal{M}(\theta^*) \equiv \{\tau(\ell)S(\cdot,\theta) \mid \ell \in \mathbf{R}, |\theta| < \theta^*\}$ for some positive constant θ^*.

Proposition 4. *There exits a neighborhood $\mathcal{U}_N(\in X)$ of $\mathcal{M}(\theta^*)$ such that any $\mathbb{U} \in \mathcal{U}_N$ is represented as*

$$\mathbb{U} = \tau(\ell)\{S(\cdot;\theta) + \mathbb{V}\}$$

by uniquely determined $(\ell, \theta, \mathbb{V})$ satisfying $\ell \in \mathbf{R}$, $|\theta| < \theta^*$ and $\mathbb{V} \in E^\perp$.

For the proof, refer to the article [6].

Here we modify this $\mathbb{V}(\in E^\perp)$ to $\theta^2\rho + \eta\zeta + \mathbb{V}$ satisfying $\rho, \zeta, \mathbb{V} \in E^\perp$ in order to get higher order equations on a center manifold. $\rho, \zeta \in E^\perp$ will be determined uniquely. By using this unique expression, we rewrite the equation (38) to that of $(\ell, \theta, \mathbb{V})$ by

$$\mathbb{U}(z,t) = \tau(\ell(t))\{S(z;\theta(t)) + \theta^2(t)\rho(z) + \eta\zeta(z) + \mathbb{V}(z,t)\}$$

for $\ell \in \mathbf{R}, |\theta| < \theta^*$ and $\mathbb{V} \in E^\perp$.

Let X^ω be the fractional powered space of X with respect to $\mathcal{L}(r_0)$ such that X^ω is imbedded into $BU^1(\mathbf{R})$, where $BU^1(\mathbf{R})$ is the functional space of continuous and bounded functions on $\mathbf{R}$ up to their first derivative. Now we are ready to state the following theorem which characterize the dynamics of the UVP/N-TW solution in the generic case (I).

Theorem 6.3. (Generic case (I)) *Let $\mathbb{U}(t)$ be a solution of (38). There exists positive constants C_0, θ^*, η^* and a neighborhood $\mathcal{U}_N$ of $\mathcal{M}(\theta^*)$ such that if the initial data $\mathbb{U}(0) \in \mathcal{U}_N$, then there exists functions $\ell(t)$ and $\theta(t)$ such that*

$$||\mathbb{U}(t,z) - \tau(\ell(t))\{P(z) + \theta(t)\Psi(z) + \theta^2(t)\rho(z)\}||_\omega \leqq C_0(|\theta(t)|^3 + |\eta|^{3/2}) \tag{43}$$

hold true as long as $|\theta(t)| < \theta^*$ and $|\eta| < \eta^*$, where $\ell(t)$ and $\theta(t)$ are estimated as

$$\begin{aligned} \dot{\ell} &= \theta + \alpha\theta^2 + O(|\theta|^3 + |\eta|^{3/2}), \\ \dot{\theta} &= \theta\eta - M_1\theta^2 - M_2\theta^3 + |\theta|O(|\theta|^3 + |\eta|^{3/2}), \end{aligned} \tag{44}$$

by particular function $\rho(z) \in E^\perp$ and constants α , M_1 and M_2 .

We will leave the proof to another paper [7] and give an expression only for M_1 which is a key coefficient to characterize the bifurcation structure in the following subsection 6.3.

$$M_1 = -\langle \frac{1}{2}\mathbb{F}''(P)\Psi^2 + \Psi_z, \Phi^*\rangle. \tag{45}$$

6.2. **Reduction to a center manifold in the non-generic case.** Next we consider the non-generic case (II), that is, $\langle b_{13}Uu^* + b_{23}Vv^*, w_0\rangle = 0$. (H2) and (H4) are replaced by (H2)' and (H4)', respectively.

(H2)' At $r = r_0$, there exists an eigenfuntion $\Psi(z)$ of $\mathcal{L}(r_0)$ satisfying

$$\mathcal{L}(r_0)\Psi(z) = 0. \tag{46}$$

(H4)' For the adjoint operator $\mathcal{L}^*(r_0)$, there exist eigenfuctions $\Phi^*(z)$ and $\Psi^*(z)$ satisfying

$$\mathcal{L}^*(r_0)\Phi^*(z) = \mathbf{0},\ \mathcal{L}^*(r_0)\Psi^*(z) = 0. \tag{47}$$

We can show the following lemma:

Lemma 6.4. *Ψ^* is uniquely determined by the normalization*

$$\langle P_z, \Psi\rangle = 0,\ \langle P_z, \Psi^*\rangle = 1 = \langle \Psi, \Phi^*\rangle,\ \langle \Psi, \Psi^*\rangle = 0 = \langle P_z, \Phi^*\rangle,$$

but Ψ and Φ^* are unique without the same one free parameter.

For the proof see the appendix. Under the conditions (H1), (H2)', (H3) and (H4)', we can similarly consider the center manifold reduction. Now we state the following theorem which characterize the dynamics of the UVP/N-TW solution in the non-generic case (II).

Theorem 6.5. (Non-generic case (II)) *Let $\mathbb{U}(t)$ be a solution of (38). There exist positive constants C_0, θ^*, η^* and a neighborhood $\mathcal{U}_N$ of $\mathcal{M}(\theta^*)$ such that if the initial data $\mathbb{U}(0) \in \mathcal{U}_N$, then there exist functions $\ell(t)$ and $\theta(t)$ such that*

$$||\mathbb{U}(t,z) - \tau(\ell(t))\{P(z) + \theta(t)\Psi(z) + \theta^2(t)\rho(z)\}||_\omega \leqq C_0(|\theta(t)|^3 + |\eta|^{3/2}) \tag{48}$$

hold true as long as $|\theta(t)| < \theta^*$ and $|\eta| < \eta^*$, where $\ell(t)$ and $\theta(t)$ are estimated as

$$\begin{aligned} \dot{\ell} &= \alpha'\theta^2 + O(|\theta|^3 + |\eta|^{3/2}), \\ \dot{\theta} &= \theta\eta - M_1'\theta^2 - M_2'\theta^3 + |\theta|O(|\theta|^3 + |\eta|^{3/2}), \end{aligned} \tag{49}$$

by particular function $\rho(z) \in E^\perp$ and constants α', M_1' and M_2'.

We will also leave the proof to another paper [7] and give an expression for M_1' which is a key coefficient to characterize the bifurcation structure in the following subsection 6.3.

$$M_1' = -\langle \frac{1}{2}\mathbb{F}''(P)\Psi^2, \Phi^*\rangle. \tag{50}$$

6.3. **Numerical calculation of the normal form coefficients.** When we ignore the higher order terms in (44) or (49), we can obtain the reduced ODE systems

$$(\text{generic case (I)}) \begin{cases} \dot{\ell} &= \theta + \alpha\theta^2, \\ \dot{\theta} &= \theta\eta - M_1\theta^2 - M_2\theta^3, \end{cases} \tag{51}$$

and

$$(\text{non} - \text{generic case (II)}) \begin{cases} \dot{\ell} &= \alpha'\theta^2, \\ \dot{\theta} &= \theta\eta - M_1'\theta^2 - M_2'\theta^3, \end{cases} \tag{52}$$

respectively. And the essential part of them is the equation for θ which characterize the w-amplitude of the UVP/N-TW solution. If M_1 or M_1' is not zero we can conclude the bifurcation structure is trans-critical. Therefore let us first focus our attention to these coefficients M_1 and M_1'.

By the discussion in Section 4 we know that there exists the critical value $r_0 > 0$ such that the linear operator L_3 in (16) has 0 as the simple maximal eigenvalue

when $r = r_0$. And it turns out numerically that $r_0 \approx 5.359$ in this parameter set in (34) and (35). In the case of (36) we know the exactly $r_0 = 5$. We are interested in the bifurcation structure around $r = r_0$. Now, the theorems 3.3 and 3.5 say that the bifurcation structure depends on the parameters b_{13}, b_{23} and is classified into two cases: (A) non-generic case : $b_{23} = \delta b_{13}$ and (B) generic case : $b_{23} \neq \delta b_{13}$, where $\delta = -\langle Uu^*, w_0\rangle / \langle Vv^*, w_0\rangle$.

We discretize the sufficiently long interval $z \in (-20, 20)$ by the mesh size $\Delta z = 0.1$ to numerically calculate all the eigenfunctions except $\Phi(z) = P_z(z)$, which we already know, and obtain $\delta \approx 0.929761$ in the case of (36). In the symmetric case we know $\delta = 1$. We take the 0-eigenfunction w_0 for the scaler linear operator L_3 positive which is the requirement noticed in subsection 3.1.

Let us first consider the generic case. Then, here are the list of eigenfunctions which is necessary for the calculation of the normal form coefficients:

- w_0 : 0-eigenfunction of $L_3(r_0)$ taken to be positive.
- w_0^* : 0-eigenfunction of $L_3^*(r_0)$ normalized by $\langle w_0, w_0^*\rangle = 1$.
- (U_z, V_z) : 0-eigenfunction for L.
- (u^*, v^*) : 0-eigenfunction for L^*.
- $\Phi = (U_z, V_z, 0)$: 0-eigenfunction for $\mathcal{L}$.
- $\Psi_0 = (Q, c_1 w_0)$: generalized 0-eigenfunction for $\mathcal{L}$.
- $\Phi_0^* = (0, 0, w_0^*)$: 0-eigenfunction for $\mathcal{L}^*$.
- $\Psi_0^* = (u^*/\gamma, v^*/\gamma, \hat{w}^*)$: generalized 0-eigenfunction for $\mathcal{L}^*$.

Notice that it is necessary to solve inhomogeneous equations:

$$LQ(z) = {}^t(c_1 b_{13} U(z) w_0(z) - U_z(z), c_1 b_{23} V(z) w_0(z) - V_z(z)), \tag{53}$$

$$L_3^*(r_0)\hat{w}^*(z) = (b_{13} U(z) u^*(z) + b_{23} V(z) v^*(z))/\gamma - w_0^*(z) \tag{54}$$

in the processes of calculating generalized eigenfunctions. Here, two constants c_1 and γ are determined by (24) and (25), respectively. We use singular value decomposition to numerically solve Q and $\hat{w}^*$. We show the graphs of these functions in figures 15, 16 , 17 and 18. Notice that Q and $\hat{w}^*$ depend on the parameters b_{13} and b_{23}. Therefore we show the graph of these functions when $b_{13} = 0.1$ and $b_{23} = 0.7$ as an example.

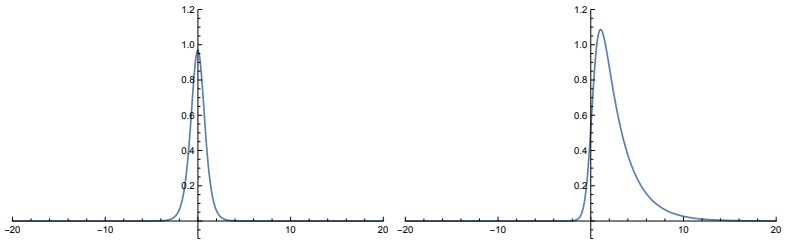

FIGURE 15. An eigenfunction w_0 (left) for L_3 and the normalized adjoint eigenfunction w_0^* (right).

In the non-generic case, two linearly independent eigenfunctions for $\mathcal{L}$ and $\mathcal{L}^*$ are given by the followings:

- $\Phi = (U_z, V_z, 0)$: 0-eigenfunction for $\mathcal{L}$.
- $\Psi_0 = (Q, w_0)$: 0-eigenfunction for $\mathcal{L}$.
- $\Phi_0^* = (0, 0, w_0^*)$: 0-eigenfunction for $\mathcal{L}^*$.

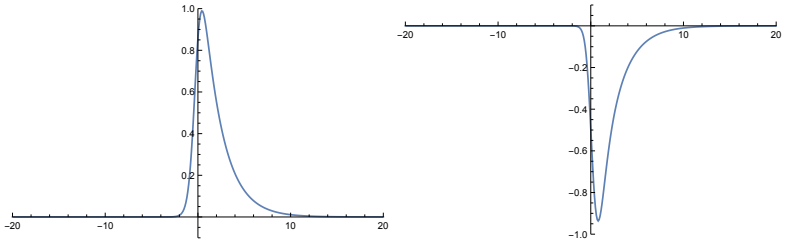

FIGURE 16. Components u^*(left) and v^*(right) of an eigenfunction for L^*.

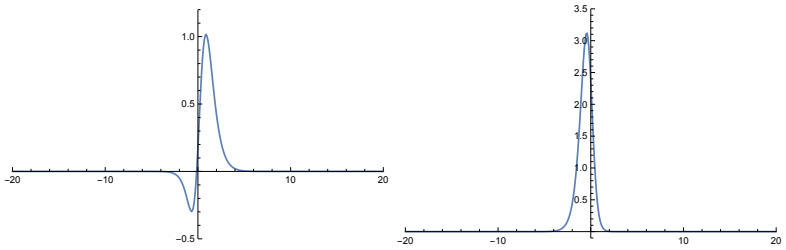

FIGURE 17. The component Q of a generalized eigenfunctionΨ_0 for $\mathcal{L}$ when $b_{13} = 0.1$ and $b_{23} = 0.7$.

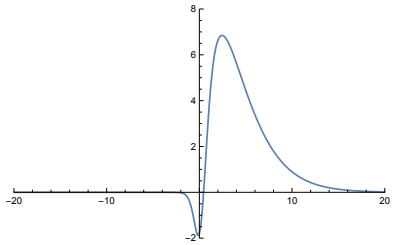

FIGURE 18. The component $\hat{w}^*$ of a generalized eigenfunctionΨ_0^* for $\mathcal{L}^*$ when $b_{13} = 0.1$ and $b_{23} = 0.7$.

- $\Psi_0^* = (u^*, v^*, \hat{w}^*)$: 0-eigenfunction for $\mathcal{L}^*$.

We need to solve the following inhomogeneous equations:

$$LQ(z) = {}^t(b_{13}U(z)w_0(z), b_{23}V(z)w_0(z)), \tag{55}$$

$$L_3^*(r_0)\hat{w}^*(z) = b_{13}U(z)u^*(z) + b_{23}V(z)v^*(z). \tag{56}$$

We also use singular value decomposition to numerically solve Q and $\hat{w}^*$. After normalizing these eigenfunctions along the lemmas 6.1 and 6.4 we calculate M_1 and M_1'.

First, let us introduce the result in the symmetric case which corresponds to the numerical continuation in Section 5.2. We describe the signs of c_1 and M_1 in the (b_{13}, b_{23})-plane (Figure 19). It should be noted that the non-generic line is the separator for the signs of both coefficients. Moreover, the parameter plane is divided into four different regions for M_1 by two lines: the non-generic line and another line which we call *pitchfork* line. We also show the grapf of M_1' along the generic line

(Figure 20). Notice that $\delta = 1$ in the symmetric case. It should be remarked that the zero point of M_1' coincides with the intersection between the two lines.

Second, Figures 21 and 22 correspond to the numerical continuation in Section 5.3. The non-generic line again separates the signs of both coefficients. And the parameter plane is similarly divided into four different regions for M_1 by two lines: the non-generic line and the pitchfork line. The zero point of M_1' also coincides with the intersection.

Since the dynamics around the bifurcation point is governed by the reduced ODE system (51), the bifurcation structure of the traveling wave solution depends basically on zero points of the second equation of this system:

$$\theta\eta - M_1\theta^2 - M_2\theta^3 = 0. \tag{57}$$

Let us denote the nontrivial solution for (57) as $\theta(\eta)$. Then $\theta(\eta)$ satisfies $\eta - M_1\theta(\eta) - M_2\theta(\eta)^2 = 0$ and $\theta(0) = 0$. Therefore, it holds that $\theta'(0) = 1/M_1$. It should be also noticed that the w-component of the leading term for the center manifold reduction is $\theta(\eta)c_1 w_0$ in the generic case. Therefore we need to take the sign of c_1 into account to determine the bifurcation curve for the peak/bottom height of w. In fact, if $c_1\theta'(0)$ is positive (negative) the bifurcation type is super-critical (sub-critical), respectively. Therefore we can conclude that the bifurcation structure is super-critical when the parameter (b_{13}, b_{23}) is below the pitchfork line. Therefore we named the line *pitchfork*. Notice that we don't claim yet that the pitchfork bifurcation really takes place in this case since we need to know $M_2 \neq 0$. This is, however, still under investigation.

On the other hand, the first equation for the reduced ODE systems (51) means the difference of the velocities between the UVP-TW and UV0-TW solutions. Let us denote this difference as $\kappa(\eta) := \theta(\eta) + \alpha\theta(\eta)^2$. It holds that $\kappa'(0) = \theta'(0) = 1/M_1$.

We summarize the above observations as follows:

Proposition 5. *The following properties on the bifurcation structure around the bifurcation point $r = r_0$ of the UVP/N-TW solution hold in the generic case.*

- *The bifurcation takes place super-critically when $c_1 \cdot M_1 > 0$. Thus, the w-component of the bifurcated solution is positive for $r > r_0$ and the velocity of this traveling wave solution is larger/smaller than that of the UV0-TW when c_1 is positive/negative, respectively. Moreover, the UVP-TW wave solution is locally asymptotically stable up to phase shift.*
- *The bifurcation takes place sub-critically when $c_1 \cdot M_1 < 0$. Thus, the w-component of the bifurcated solution is positive for $r < r_0$ and the velocity of this traveling wave solution is larger/smaller than that of the UV0-TW when c_1 is positive/negative, respectively. Moreover, the UVP-TW solution is unstable.*

Second, let us consider the non-generic case. Similarly to the generic case, the dynamics around the bifurcation point is governed by the reduced ODE system (52), the bifurcation structure of the traveling wave solution depends basically on zero points of the second equation of this systems. Although, this is equivalent to (57), the coefficients M_1', M_2' are different from the generic case and the basis for the center manifold reduction are different. However, the nontrivial solution $\theta(\eta)$ for (57) satisfies $\eta - M_1'\theta(\eta) - M_2'\theta(\eta)^2 = 0$ and $\theta(0) = 0$ similarly to the generic case. And therefore, it holds that $\theta'(0) = 1/M_1'$. It should be also noticed that the w-component of the leading term for the center manifold reduction is $\theta(\eta)w_0$ in the

non-generic case. Therefore, the bifurcation type is super-critical (sub-critical), if $\theta'(0)$ is positive (negative), respectively.

To summarize, we have the following proposition:

Proposition 6. *The following properties on the bifurcation structure around the bifurcation point $r = r_0$ of the UVP/N-TW solution hold in the non-generic case.*

- *The bifurcation takes place super-critically when $M_1' > 0$. Thus, the w-component of the bifurcated solution is positive for $r > r_0$.*
- *The bifurcation takes place sub-critically when $M_1' < 0$. Thus, the w-component of the bifurcated solution is positive for $r < r_0$.*

Notice that the bifurcation structure is super-critical if the point (b_{13}, b_{23}) is below the pitchfork line whether it's on a generic line or not. And the traveling velocity of the UVP-TW is faster/slower than that of the UV0-TW if the point (b_{13}, b_{23}) is below(above) the non-generic line. We can thus confirm all the results of numerical continuations in subsections 5.2 and 5.3 are consistent with this explanation by using the reduced equation.

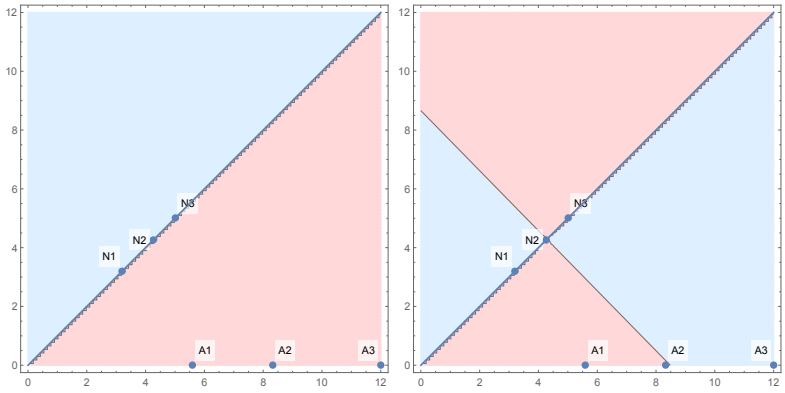

FIGURE 19. Signs of c_1(Left) and M_1(Right) for the system (35) in subsection 5.2 are shown by red(positive) and blue(negative) in the (b_{13}, b_{23})-plane.

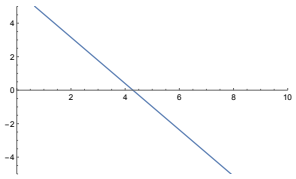

FIGURE 20. Graph of M_1' with respect to b_{13} along the generic line of $b_{23} = b_{13}$ for the system (35).

7. **Discussion.** The stability and bifurcation for the front traveling wave solution between two competing species were studied by adding a third species which is also competing with the original two. We have prepared representative examples where the original traveling wave solution loses its stability by changing the growth

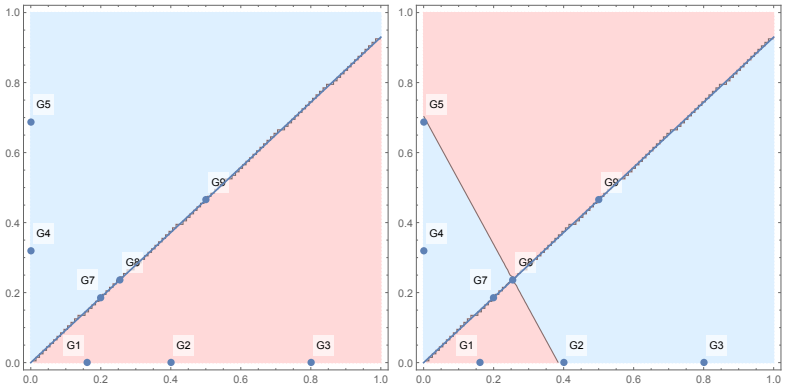

FIGURE 21. Signs of c_1(Left) and M_1(Right) for the system (36) in subsection 5.3 are shown by red(positive) and blue(negative) in the (b_{13}, b_{23})-plane.

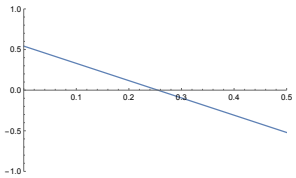

FIGURE 22. Graphs of M_1' with respect to b_{13} along the line of $b_{23} = \delta b_{13}$for the system (36).

rate for the third species. We also showed the bifurcation structures by using numerical continuation. The bifurcation point is determined only by the original traveling wave and the inter-species interactions with the third species from the original two. On the other hand, the bifurcation structures depend on the inter-species interactions with the original two species back from the third. In fact, we observed super- and sub-critical bifurcations depending on these interactions, and found that the velocity change of the bifurcated traveling wave also depends on the interactions.

We then examined the bifurcation structure by using a center manifold reduction around the critical point. It is, however, not an easy task since this problem is the bifurcation of a traveling wave and therefore the eigenspace corresponding to this critical point is degenerate. By using a method explored by one of the authors [6] we have obtained the normal form which characterizes the reduced dynamics. The process of deriving the reduced dynamics is too heavy to be included in this study, so the details are given in [7]. We instead, focus on calculating the normal form coefficients and performing collation between the continuation results. It turns out that the parameter space can be classified by the sign of the quadratic coefficient of the normal form. This classification determines the local bifurcation structure. Of course, this classification was obtained by numerical calculation, so we look forward to future analysis as to why such boundaries appear.

This is also related to the global bifurcation structure. It should be noted that the branch of UVP-TW solution exist only up to certain value r^* of the growth

rate r. When r approaches to r^*, UVP-TW seems to converge to another front traveling wave solutions between W and U, or W and V. Therefore the branch of the UVP-TW looks almost vertical when the UVP-TW approaches to these different traveling waves. Also the limit point r^* changes forward and backward, depending on (b_{13}, b_{23}). We show the change of bifurcation branches by moving (b_{13}, b_{23}) almost along the pitchfork line in Figure 23. For this reason we can observe bistable hysteresis between UVP-TW and UV0-TW when (b_{13}, b_{23}) is far from the non-generic line. Therefore we expect the heteroclinic gluing bifurcation [2] will be a key in understanding the global bifurcation, although it is still an open question.

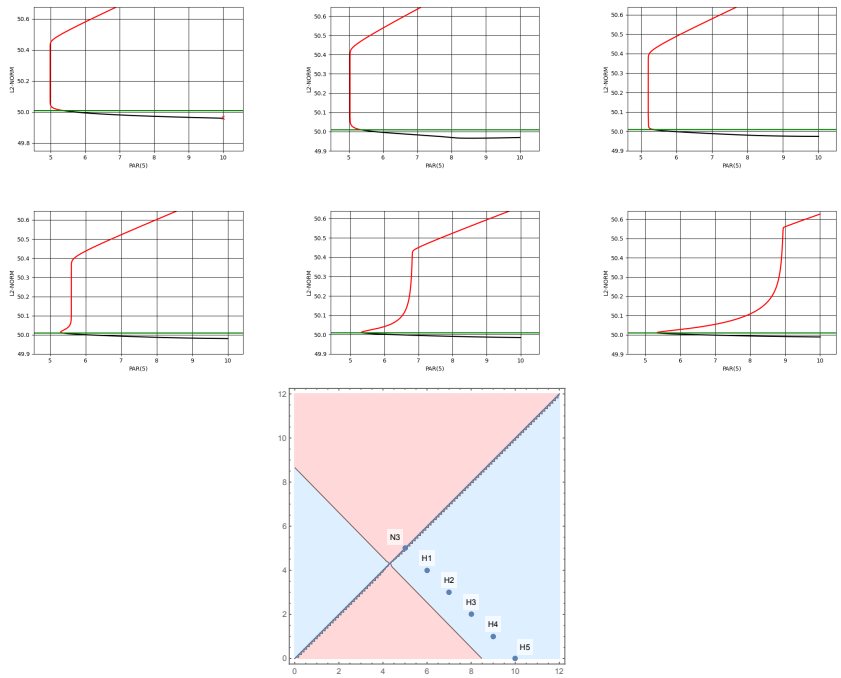

FIGURE 23. Bifurcation diagrams of UV0-SS(green), UVP-SS(red) and UVN-SS(black) for (35) with respect to r when $(b_{13}, b_{23}) = (5,5), (6,4), (7,3), (8,2), (9,1), (10,0)$ (N3, H1, H2, H3, H4, H5) from the left. These points are all right after crossing the pitchfork line. Notice that diagonal segment on the red curve is no longer the UVP-SS but traveling wave solutions between W and U or W and V. Signs of M_1(below) are also shown in the (b_{13}, b_{23})-plane.

8. **Appendix.** Here, we write the proof of lemmas for the normalization of eigenfunctions in Section 6.1 and 6.2.

Proof of Lemma 6.1. Though this proof is not difficult, we give it shortly because we want to refer to it later on. An eigenfunction and generalized eigenfunctions stated in Theorem 3.3 are not unique. So, we specify these eigenfunction and generalized eigenfunctions stated in Theorem 3.3 with the sub index 0. That is,

$$\mathcal{L}(r_0)\Psi_0(z) = -P_z(z),\ \mathcal{L}^*(r_0)\Phi_0^*(z) = \mathbf{0},\ \mathcal{L}^*(r_0)\Psi_0^*(z) = -\Phi_0^*(z). \tag{58}$$

Any eigenfunction $\Phi^*(z)$ and generalized eigenfunctions $\Psi(z), \Psi^*(z)$ satisfying the relations stated in Theorem 3.3 are represented as follows:

$$\Psi(z) = \Psi_0(z) + k_1 P_z(z),\ \Phi^*(z) = k_2 \Phi_0^*(z),\ \Psi^*(z) = k_2 \Psi_0^*(z) + k_3 \Phi_0^*(z) \tag{59}$$

for any constants k_1, k_2 and k_3. So, substituting these into the normalization in Lemma 6.1, we easily find that

$$\begin{aligned} &k_1 = -\langle P_z, \Psi_0(z)\rangle / \langle P_z, P_z\rangle, \quad k_2 = 1/\langle P_z, \Psi_0^*\rangle, \\ &k_3 = \{-k_1 - k_2 \langle \Psi_0, \Psi_0^*\rangle\} / \langle \Psi_0, \Phi_0^*\rangle \end{aligned} \tag{60}$$

are determined uniquely. Specifically $\langle P_z, \Psi_0^*\rangle = \langle {}^t(U_z, V_z), {}^t(u^*, v^*)\rangle/\gamma$, where γ is defined by (25). So, $k_2 = \gamma / \langle {}^t(U_z, V_z), {}^t(u^*, v^*)\rangle$. Thus the proof is completed. □

Proof of Lemma 6.4. Though this proof is not difficult, we give it shortly because we want to refer to it later on. Eigenfunctions stated in Theorem 3.5 are not unique. So, we specify these eigenfunctions stated in Theorem 3.5 with the sub index 0. That is,

$$\mathcal{L}(r_0)\Psi_0(z) = \mathbf{0},\ \mathcal{L}^*(r_0)\Phi_0^*(z) = \mathbf{0},\ \mathcal{L}^*(r_0)\Psi_0^*(z) = \mathbf{0}. \tag{61}$$

Any eigenfunctions $\Phi^*(z), \Psi(z), \Psi^*(z)$ satisfying the relations stated in Theorem 3.5 are represented as follows:

$$\begin{aligned} &\Psi(z) = \ell_1 P_z(z) + \ell_2 \Psi_0(z), \quad \Phi^*(z) = m_1 \Phi_0^*(z) + m_2 \Psi_0^*(z), \\ &\Psi^*(z) = n_1 \Phi_0^*(z) + n_2 \Psi_0^*(z) \end{aligned} \tag{62}$$

for any constants $\ell_1, \ell_2, m_1, m_2, n_1$ and n_2. So, substituting these into the normalization in Lemma 6.4, we easily find that

$$\begin{aligned} &\ell_1 = -\ell_2 \langle P_z, \Psi_0(z)\rangle / \langle P_z, P_z\rangle, \\ &m_1 = 1/(\ell_2 \langle \Psi_0, \Phi_0^*\rangle) = 1/\ell_2, \quad m_2 = 0, \\ &n_1 = \{\langle P_z, \Psi_0\rangle / \langle P_z, P_z\rangle - \langle \Psi_0, \Psi_0^*\rangle / \langle P_z, \Psi_0^*\rangle\} / \langle \Psi_0, \Phi_0^*\rangle, \\ &n_2 = 1/\langle P_z, \Psi_0^*\rangle \end{aligned} \tag{63}$$

are determined with any constant ℓ_2. Then Ψ^* is uniquely determined but Ψ, Φ^* depend on the free constant ℓ_2. Thus the proof is completed. □

Acknowledgment. This work is based on discussions with Professor Masayasu Mimura, who passed away in 2021. We would like to express our deep gratitude for his important suggestions. This work would not have been possible without his strong encouragement.

REFERENCES

[1] H. Berestycki, O. Diekmann, C.J. Nagelker and P.A. Zegeling, Can a species keep pace with a shifting climate?, *Bulletin of Mathematical Biology*, **71** (2009), 399–429.

[2] C.-H. Chang and C.-C. Chen, Existence of Front-Back-Pulse Solutions of a Three-Species Lotka-Volterra Competition-Diffusion System, Journal of Dynamics and Differential Equations, https://doi.org/10.1007/s10884-021-10090-6 , 2021

[3] C.-H. Chang, C.-C. Chen, L.-C. Hung, M. Mimura and T. Ogawa, Existence and stability of non-monotone travelling wave solutions for the diffusive Lotka-Volterra system of three competing species, *Nonlinearity*, **33(10)**, 2020, 5080-5110

[4] C.-C. Chen, L.-C. Hung, M. Mimura and D. Ueyama, Exact travelling wave solutions of three-species competition-diffusion systems, Discrete and Continuous Dynamical Systems - Series B, 2012 vol: 17 (8) pp: 2653-2669

[5] E. J. Doedel, B. E. Oldeman, A. R. Champneys, F. Dercole, T. F. Fairgrieve, Y. Kuznetsov, R. C. Paffenroth, B. Sandstede, X. J. Wang and C. H. Zhang, "AUTO-07p: Continuation and Bifurcation Software for Ordinary Differential Equations," Concordia Univ., Version 0.7, 2010. Available from: http://sourceforge.net/projects/auto-07p/files/auto07p/.

[6] S.-I., Ei, The motion of weakly interaction pulses in reaction-diffusion systems, *J. Dynam. Diff. Eq.*, **14** (2002), 85–137.

[7] S.-I., Ei, H. Ikeda and T.Ogawa, Bifurcation of co-existing traveling wave solutions in a three-component competition-diffusion system, Physica D **448** (2023), 133703.

[8] M. W. Hirsch, Stability and convergence in strongly monotone dynamical systems, *J. Reine Angew. Math.*, **383** (1988), 1–53.

[9] Y. Kan-on, Parameter dependency of propagation speed of travelling waves for competition-diffusion equations, *SIAM J. Math. Anal.*, **26** (1995), 430–463.

[10] Y. Kan-on and Q. Fang, Stability of monotone travelling waves for competition-diffusion equations, *Japan J. Indust. Appl. Math..*, **13** (1996), 343–349.

[11] Y. Kan-on and E. Yanagida, Existence of non-constant stable equilibria in competition-diffusion equations, *Hiroshima Math. J.*, **33** (1993), 193–221.

[12] K. Kishimoto and H. F. Weinberger, The spatial homogeneity of stable equilibria of some reaction-diffusion systems on convex domains, *J. Differential Equations*, **58** (1985), 15–21.

[13] M. Rodrigo and M. Mimura, Exact solutions of a competition-diffusion system, Hiroshima Math. J., 30 (2000), 257-270.

[14] M. Rodrigo and M. Mimura, Exact solutions of reaction-diffusion systems and nonlinear wave equations, Japan J. Indust. Appl. Math., 18 (2001), 657-696.